DEVELOPMENT OF LAND-USE MAP FOR SALT RIVER BASIN

USING SATELLITE IMAGERY

A Thesis

presented to

the Faculty of the Graduate School

at the University of Missouri

In Partial Fulfillment

of the Requirements for the Degree

of Master of Science

---

by

ANH THI TUAN NGUYEN

Allen Thompson, Thesis Supervisor

DECEMBER 2010

The undersigned, appointed by the Dean of the Graduate School, have examined the thesis entitled:

DEVELOPMENT OF LAND-USE MAP FOR SALT RIVER BASIN

USING SATELLITE IMAGERY

Presented by Anh Nguyen Thi Tuan

a candidate for the degree of Master of Science

and hereby certify that in their opinion it is worthy of acceptance

_____

Thompson Allen, Biological Engineering Department

_____

Kenneth Sudduth, Biological Engineering Department

_____

Cuizhen (Susan) Wang, Geography Department

ACKNOWLEDGEMENTS

I would like to thank my committee for their encouragement and enthusiasm throughout my time at the University of Missouri. My research would not have been possible without the help and support of many people. I am grateful to my advisor, Dr. Allen Thompson, for encouraging this work and his support of my effort. To my committee members: Dr. Ken Sudduth and Cuizhen Wang for their willing guidance and remote sensing expertise. Financial support was provided by the MOET program that gave me the opportunity to study in the Biological Engineering Department.

I wish to express gratitude to Prof. Joseph Hobbs for his encouragement and support through the duration of my studies. I also wish to thank the staff at the University of Missouri Columbia for their assistance, advice and guidance through my academic program. My efforts have been influenced by many instructors in the departments of Biological Engineering, Geography and Forestry with whom I have completed course-work during my past two and half years. My knowledge and abilities have been greatly enhanced by their efforts.

I wish to express my special thanks and gratitude to Daniel Seidel, Dylan Caspari, Josh Kezer, Jared Caspari, Jean Elizabeth, Trang Tran, Truc Bui, Anh Phan, Quang Nguyen, Giang Nguyen, BaoAnh Nguyen, Dung Tran and Nguyen Doan for their understanding, sharing, and support throughout the duration of my studies at the University of Missouri.

I would like to thank all the staff at the International Center for their help, support and promoting the chance to experience American education and culture firsthand and to share

my own cultures. Thanks for providing a variety of workshops, events, volunteer opportunities and outreach programs and involving me with the global campus.

Finally, this thesis would not have been possible without the constant support and encouragement of my parents and my family. I thank my parents, my sister Nguyet Nguyen and my brother Tuan Nguyen for believing in me and encouraging me to study abroad.

TABLE OF CONTENTS

LIST OF TABLES

Table Page

LIST OF FIGURES

Figure Page

DEVELOPMENT OF LAND-USE MAP FOR SALT RIVER BASIN

USING SATELLITE IMAGERY

Anh Nguyen

Allen Thompson, Thesis Supervisor

ABSTRACT

The Salt River watershed is located in northeastern Missouri. Outflows from the watershed drain into Mark Twain Lake, the major water supply source for people in the region. Since most of the land use in the watershed is cropland and grass, an evaluation for possible improvement of watershed management is encouraged. However, there is a lack of field/survey information concerning the crops in previous years necessary to build a long term simulation and to validate the long term trend of pollutant concentrations. A potential method to aid land-use evaluation is the use of satellite imaging data. Satellite remote sensing data have many advantages compared with other data sources, such as field methods, or aerial photography and have been widely used in land cover classification. It provides the capability to evaluate dynamic landscape pattern and observe changes and trends across a large scale pattern through time. The overall objective of this study was to apply Landsat 5 Thematic Mapper (TM) data to build crop type maps for Salt River Basin for a two-year period (2005-2006) useful in evaluating land-use management. Decision tree analysis, combination of pixel and object based methods, was applied. Ground truth data in Goodwater creek sub-basin and Greenley reference area were used to assess the accuracy of the procedure, and crop acreage estimates were compared to county-level statistics. Crop type classification of 2005 had higher accuracy than that of 2006 because there was more in-season Landsat data obtained in 2005. However, this method was efficient in classifying crops when there was lack of cloud-free images in growing season with an overall accuracy was 90% in 2006. Additional testing of this method could result in a robust technique for crop classification for specific crops in cloud-free-limited Landsat data for applying to other study.

Chapter 1

INTRODUCTION

The Salt River basin is located in northeastern Missouri. The closing of Clarence Cannon Dam in 1983 formed the Mark Twain Lake. The total catchment area is approximately 6417 km^2. River and stream outflow from the watershed drain into Mark Twain Lake, the major water supply source for people in the region. Since the dam was closed, the Lake has been receiving sediment in the watershed, including inorganic sediment loading, which can degrade water quality. Concerning these soil and water quality problems, the Salt River was selected as one of the USDA Agricultural Research Service benchmark watersheds for Conservation Effects Assessment Project (CEAP) (Lerch et al, 2008). Since most of the land use in the watershed is cropland and grass, an evaluation for improvement of watershed management is possible. Previous research in the watershed area included quantifying the nutrient and sediment concentrations in five major tributaries in the Upper Salt River Basin and ten small tributaries in the Middle Fork of the Salt River (Skadeland, 1992) ; applying Remote Sensing of Suspended solid and Turbidity in Mark Twain Lake, Missouri (Allen, 2000). Ghidey et al. (2005) had built a model to simulate hydrology and water quality for a claypan soil watershed and scaled up the SWAT (Soil and Water Assessment Tool) model from Goodwater Creek (Ghidey et al, 2007). Results from the SWAT model showed that the simulation model can be used for a long term estimation of contaminant concentration. However, there is a lack of field/survey information concerning the crop types that were planted in previous years in order to build a long term simulation model and to validate the long term trend of pollutant concentrations. Land use is an

important input to the SWAT model. Cropland Data Layer (CDL) produced by National Agricultural Statistic Service (NASS), based on NASS annual sampling data. Thus, the requirement to develop a crop map for the watershed area is justified, especially for the previous years.

Since satellite remote sensing data have many advantages compared with other data sources, such as field methods, and aerial photography, it has been used widely in land cover classification. It is useful in evaluating temporal and spatial effects. Temporal effects show the change of feature spectral characteristics over time. Spatial effects help to analyze factors with a similar characteristic feature at a given point of time but at different geographic locations. The other advantage of remote sensing is that it can offer cost-effective means of providing more frequent crop/land cover data for short and long term planning. It provides the capability to evaluate dynamic landscape patterns and to observe changes and trends across a large scale pattern through time. It also provides spatially and temporally comprehensive data (Franklin, 2001; Jensen, 2005). Using the information from remote sensing satellites properly would be very useful for managers to be able to understand natural impacts and to solve many environmental issues. The advantage of difference in spectral of objects can help to discriminate between objects in the area. However, there are several factors that can affect a feature's reflectance. Remote sensing techniques provide a synoptic view of an area and methods utilizing remote sensing data in deterministic models can potentially supply new information.

The purpose of this study is to apply Landsat 5 Thematic Mapper (TM) data to build crop type maps for the Salt River Watershed for two previous years (2005- 2006). The study also applies the Normalized Difference Vegetation Indices derived from MODIS as a

reference to build the hypothesis for differentiating among crop types during the growing season.

1.1 Research objectives

The overall objective of this study was to develop land cover/land use maps for Salt River basin from remote sensing data. Specifically, the objectives were to:

- Find the most appropriate method to delineate crop types in the agricultural land in Salt River basin under conditions of limited field data.
- Analyze and determine crop phenological behaviors in Salt River basin.
- Develop land cover maps from this watershed area for years 2005 and 2006

Chapter 2

LITERATURE REVIEW

2.1 Remote Sensing

Applying satellite remote sensing data is the process of analyzing data from satellite, which collects spectral information about an object, area, or phenomenon without contacting the object, area, or phenomenon. Satellite imagery uses electromagnetic energy sensors to obtain reflectance data from features on earth.

Remote sensors collect radiation reflectance from features at a distance which crosses through a path length of the atmosphere and is affected by atmospheric scattering and absorption. Atmospheric scattering is the unpredictable reflectance of radiation by particles in the atmosphere (Rayleigh scatter, Mie scatter, non selective scatter) (Jensen, 2000). Conversely, atmospheric absorption is the phenomena of loss energy due to atmospheric particles, such as water vapor, carbon dioxide and ozone.

Spectral reflectance of an object varies as a function of wavelength which can help to discriminate objects in the area. For example, healthy green vegetation can be classified from dry bare soil and clear lake water since water has low reflectance in visible wavelength and no reflectance in near IR wavelength, while bare soil has higher reflectance than vegetation in visible wavelength but less in the near infrared (IR) wavelength. Moreover, the healthy green vegetation spectral curve has a “peak and valley” that can be easily identified. (Lillesand, 2004) Although the reflectance of individual features varies along the spectrum, the curves exhibit some elementary points concerning spectral reflectance. Some factors affect the feature’s reflectance. For example, the near IR reflectance of vegetation increases

with the number of leaf layers in a canopy, with a maximum reflectance at about eight layers of leaves (Bauer, 1985). Soil reflectance is affected by the presence of iron oxide, organic matter content or moisture content. Soil texture and surface roughness are two factors that influence soil reflectance as well. Soil with low moisture content and coarse texture has a high reflectance, while an increase in organic content in the soil reduces reflectance. (Lillesand, 2004)

Water absorbs radiation strongly at water absorption bands, located at 1.4, 1.9 and 2.7 μm. This characteristic helps to locate and define water bodies within the area. However, the water reflectance is affected by solid material within the water. When the turbidity of water increases, reflectance also increases. Lyon et al. (1988) used the data from multiple days Landsat and AVHRR to determine suspended sediment concentration based on this feature of water reflectance. Choubey and Subramanian (1992) used data from India Remote Sensing Satellite-1A to investigate this character of water turbidity to estimate suspended solids. Thus, in order to operate efficiently, the knowledge and understanding of spectral characteristics of the particular features under investigation, as well as what factors influence these characteristics are required. Also, information about vegetation water content allows the user to infer water stress for irrigation decisions. Jackson et al. (2004) explored the potential of using remote sensing derived the normalized difference water index, to map and monitor corn and soybean.

Another advantage of satellite remote sensing data is its usefulness in evaluating temporal and spatial effects. Temporal effects show the change of feature spectral characteristics over time. Spatial effects help to analyze factors with a similar characteristic feature at a given point of time but at different geographic locations. In addition, the energy

recorded is affected by the atmosphere through which the radiation passes. Atmospheric correction models are built to correct these types of errors.

Image processing systems contain algorithms to remove or reduce atmospheric affect. The simplest and commonly used model for atmospheric correction is DOS (Dark Object Subtraction) with the assumption that atmospheric effects are the same for all pixels in the image and dark objects (clear water bodies) have homogeneously zero radiance for all bands. The procedure requires checking the visible band radiances over the lake or other dark objects and adjusting the observed value to more closely match the expected reflectance.

One of the most common applications of remote sensing is land cover classification, the process of assigning a particular class to an image object or pixels in the image (Cihlar, 2000; Foody, 2002). Land cover classification can be applied at different scales, from continental and global level scales (Friedl et al., 1999; Agrawal et al., 2003; Joshi et al., 2006) to local regional studies (Brook and Kenkel, 2002; Reese et al., 2002; Van Niel and McVicar, 2004). The Landsat imagery is commonly used for medium resolution land cover classification. Another application of crop mapping include estimating crop yield (Doraiswamy et al., 2006; Wang et al., 2005), water content (Jackson et al., 2004), crop estimation (Craig, 2001) as well as simple crop classification (Yamamoto et al., 2009). The relationship between level scale and spatial resolution in satellite-based land cover mapping is listed in Table 2.1.

2.1.1 Landsat Thematic Mapper History

The Landsat 5 Thematic Mapper (TM) and the Landsat 7 Enhanced Thematic Mapper Plus (ETM+) have repetitive, circular, sun-synchronous, near polar orbits with a 16-day

repeat cycle for each satellite. Both of them are 8-bit, moderate resolution sensor (30m resolution). In 2003, an instrument anomaly was detected onboard the satellite that collects Landsat 7 ETM+ data. The SLC failure of Landsat 7 ETM+ has forced users to rely on the Landsat 5 TM data for most Landsat image requirements. The TM sensor collects data in seven bands (Table 2.2). Both the TM mid-IR bands (bands 5 and 7) are sensitive to plant water stress (Lillesand, 2004). Plant stress classification is also aided by TM band 1. For a mapping of water sediment pattern, a normal color composite of bands 1, 2 and 3 (Blue Green Red) is preferred. For vegetation discrimination, the combination of visible bands (bands 1-3) with near IR (band 4) and mid IR (bands 5-7) are very helpful.

Table 2.1 Relationship between scale and spatial resolution in satellite-based land cover mapping programs (Franklin, 2002)

Low spatial resolution imagery	study phenomena that can vary over 100s or 1000s of meters (small scale) and could be supported with GOES, NOAA AVHRR, EOS MODIS, SPOT VEGETATION sensor data
Medium spatial resolution	study of phenomena that can vary over 10s or 100s of meters (medium scale) typically with imagery from sensors on the Landsat, SPOT, IRS, JERS, ERS, Radarsat and Shuttle platforms
High spatial resolution	study of phenomena that can vary over scales of centimeters to meters (large scale), are currently supported by aerial remote sensing platforms, IKONOS and very specific applications of coarse resolution satellite imagery (e.g., coarse pixels resolution unmixing studies)

Table 2.2 Thematic Mapper Spectral Bands (adapted from Lillesand, 2004)

Band	Wavelength (μm)	Nominal Spectral Location	Principal Application
1	0.45 – 0.52	Blue	Designed for water body penetration, making it useful for coastal water mapping. Also useful for soil/vegetation discrimination, forest-type mapping, and cultural feature identification
2	0.52 – 0.60	Green	Designed to measure green reflectance peak of vegetation for vegetation discrimination and vigor assessment. Also useful for cultural feature identification
3	0.63 – 0.69	Red	Designed to sense a chlorophyll absorption region aiding in plant species differentiation. Also useful for culture feature identification
4	0.76 – 0.90	Near IR	Useful for determining vegetation types, vigor, and biomass content, for delineating water bodies, and for soil moisture discrimination
5	1.55 – 1.75	Mid IR	Indicative of vegetation moisture content and soil moisture. Also useful for differentiation of snow from clouds
6[a]	10.4 – 12.5	Thermal IR	Useful in vegetation stress analysis, soil moisture discrimination, and thermal mapping application
7[a]	2.08 – 2.35	Mid IR	Useful for discrimination of mineral and rock types. Also sensitive to vegetation moisture content
[a]*Bands 6 and 7 are out of wavelength sequence because band 7 was added to the TM later in the original system design process*			

Landsat image interpretation has been widely used in many fields, such as agriculture, cartography, civil engineering, environmental monitoring, forestry, geography, land use planning and oceanography. However, there is a problem with applying Landsat 5 TM, because of the low temporal resolution (16 days temporal resolution). Limitation of high spatial resolution data includes data cost and infrequency.

2.1.2 Moderate Resolution Imaging Spectrometer (MODIS)

MODIS has a much wider field of view than Landsat which gives a greater swath width and also has a higher temporal resolution. For certain time-sensitive applications, such as crop mapping during the growing season, a frequent revisit cycle is very important. MODIS provides a long term observation which is very useful to enhance knowledge of global dynamics and processes (SBRC, 1994). MODIS views the entire surface of the Earth everyday. This feature of MODIS was used in many studies of large scale mapping (Doraiswamy et al., 2006; Wardlow et al., 2007; Chang, 2007). Doraiswamy et al. (2006) used MODIS Terra data at 250m resolution to classify crop area in four provinces of Brazil that are the major soybean producing area and demonstrate that MODIS imagery can be used for regional classification when screened for data anomalies and affected by clouds or compositing procedures. He also concluded that frequency of MODIS data acquisition at 250m pixel resolution can be used for operational yield prediction programs. The MODIS sensor offers an option for dealing with some mapping criteria. However, the MODIS pixel is much larger than the 30m Landsat pixels used for creating maps – therefore, merging these large pixels into the existing map would generate a significant error to the map quality.

2.2 Land cover classification

Analysis of data from satellite remote sensing is widely used, especially for land use - land cover classification. It is the process of assigning all pixels in the image to a particular class or theme based on their specific spectral information with different spectral bands from the satellite sensor. Each type of satellite has several wave bands with specific wavelengths that collect the level of reflected solar radiation. By spatially and spectrally enhancing an image, the pattern can be recognized by the human eye. Remote sensing of cropland has been used a variety of methods and techniques, including multi-temporal analysis, object-based analysis, and classification methods such as supervised and unsupervised approaches.

2.3 Methods of classification

The overall objective of classification is to categorize all pixels in an image into land cover classes. Different features have different combinations of Digital numbers (DNs) based on their spectral reflectance and emission. Applying remote sensing data to separate vegetative types is studied, especially for agricultural croplands (Franklin and Wulder, 2003). In an agriculture crop survey, distinct spectral and spatial changes during a growing season can help to discrimination multi-date imagery which is very difficult when using a single-date image, because they include different vegetation types which often show a similar spectral response, resulting from a similar leaf area index value and internal structure.

There are many different techniques to combine and analyze multi-temporal scenes (Van Niel and McVicar, 2004). Moreover, multi-temporal techniques can increase the accuracy of the classification process (Murthy et al., 2003; Van Niel and McVicar, 2004). Van Niel and McVicar (2004) also noticed that a minimum of two and preferably three

images taken over a single growing season are necessary to distinguish many different crop and grassland types. With coarse spatial resolution images and high temporal resolution as MODIS, it is possible to generate a cloud-free image for a growing season, but it's rather difficult to get cloud-free images with Landsat (30m spatial resolution 16-day temporal resolution).

There are two types of classification techniques: object-based classification and pixel-based classification. Most traditional remote sensing classification is pixel-based. Aplin and Atkinson (2001) applied the object-based classification as a method to improve accuracy.

2.3.1 Object-based versus pixel-based classification

Object-based classification divides the satellite image into an object or segments that represent a homogenous unit on the ground. The entire object is classified based on the overall statistical properties of the pixels that make up the object rather than classifying each pixel separately as in pixel-based classification (McIver and Friedl, 2002). The difficulty of object-based is the establishment of significant objects. It is not possible to hand digitize for large areas. All natural boundaries may not be found, and those found may not match real world objects. It requires a laborious set of training data and prior knowledge of the area to correctly use this method. In addition, features such as roads or streams may be included in other objects (De Wit and Clevers, 2004). Thus, it results in overestimation or underestimation of the area.

There are two main weakness of the pixel-based method. The first weakness is that the products do not express the actual landscape structure well. The second weakness is the occurrence of mixed pixels within a homogenous field and problems with the edge pixels.

Object-based classification is usually combined with other techniques and can be separated into two main types: supervised classification and unsupervised classification. The difference between these two techniques is that supervised classification involves a training step followed by a classification step (priori process). In the unsupervised classification approach, pixels are grouped based on image statistics first. Then the analyst labels these spectral groups (called clusters) by comparing the classified image data to ground reference data (post-prior process).

2.3.2 Supervised classification methods

There are two basic types of supervised classification: parametric method and non-parametric method. The commonly used parametric supervised classification is Gaussian Maximum Likelihood Classifier (MLC). The MLC quantitatively evaluates both the variance and covariance of the category spectral response pattern with the assumption that the category training data are distributed normally. The unclassified pixels from the image are assigned to the class for which they have the highest membership probability. Non-parametric methods make no assumption about statistical distribution of the data. This is the advantage of the non-parametric supervised classification method; however, it is dependent on the training data conditions. The non-parametric method includes a decision tree (Franklin et al., 2002; Jang et al., 2009). The decision tree method has some advantages (Franklin and Wulder, 2003; Chubey et al., 2006), such as:

- Possible handling high-dimension data set, include non-remotely sensed data as an aid in classification
- Possible to do with both categorical and continuous data

- No assumption about statistical distribution of data

- Has been shown to outperform both MLC and non-parametric classifiers (Chubey et al., 2006)

However, decision trees rely on the quality of the training data and knowledge about the objects and factors that affect the objects' characteristics.

2.3.3 Unsupervised classification methods

Unsupervised classifiers do not utilize training data as the basis of classification. Classes from unsupervised classification are spectral classes, because they are based on the natural groupings in the image values. The analyst compares the data with some form of reference data to determine the identity and informational value of spectral classes. There are several clustering algorithms that can be used for spectral grouping. One common form is called "K-means" approach. Each pixel is assigned to the cluster whose arbitrary mean vector is closest. After all pixels have been classified, revised mean vectors for each cluster are computed and then the revised means are used as the basis to reclassify the image data. The procedure continues until there is no significant change in the location of the class mean vector between successive iteration of the algorithm. ISODATA (Iterative Self-Organizing Data Analysis) is a widely used "K-means" method for unsupervised classification (Tou and Gozalez, 1974). This algorithm permits the number of clusters to change from iteration to the next iteration by merging, splitting and deleting clusters (Lillesand et al., 2004).

2.3.4 Ground truth data

The class maps from supervised or unsupervised classification can be validated with ground truth data. Ground truth data – reference data may be collected from measurements or

observations about the objects, area or phenomena. It can be derived from different sources. For example, it could be a survey map, laboratory report or aerial photograph. These data are used to calibrate a sensor, to verify information extracted from remote sensing data and to help in analysis and interpretation of remote sensing data. Reference data can be very expensive and time consuming to properly collect (Lillesand et al., 2004).

2.4 Vegetation indices (VI)

Before the launch of Landsat satellites, the idea of using spectral reflectance ratio of NIR (0.75 μm) to red (0.65 μm) was presented by Birth and McVey (1968), which they called the turf color index. Nowadays, formulas combining NIR and Red reflectance are commonly referred to as spectral vegetation indices. There are more than 20 vegetation indices in use. A summary of selected VI are in Table 2.3. Vegetation indices were applied to satellite remote sensing data, which is called the normalized difference vegetation index (NDVI).

2.4.1 Normalized Difference Vegetation Index (NDVI)

The Normalized Difference Vegetation Index was developed by Rouse et al. (1974) defined as

$$NDVI = [NIR - red] / [NIR + red] \quad (2.1)$$

Blair and Baumgerdner (1977) showed that the phenology of various vegetation types could be monitored with a VI data. NDVI is a single simple and easy to compare index that makes it widely used over time.

Table 2.3 Selected remote sensing Vegetation Indices (adapted from Jensen, 2000)

Vegetation Index	Equation	References
Simple Ratio (SR)	$SR = \frac{NIR}{red}$	Birth and McVey, 1968
Normal Difference Vegetation Index (NDVI)	$NDVI = \frac{NIR - red}{NIR + red}$	Rouse et al., 1974; Deering et al., 1975
Kauth-Thomas Transformation	Landsat Multispectral Scanner (MSS)	Kauth and Thomas, 1976;
Brightness	$B = 0.332_{mss1}+0.603_{mss2}+0.675_{mss3}+0.262_{mss4}$	Kauth et al., 1979
Greenness	$G = -0.283_{mss1} - 0.66_{mss2}+0.577_{mss3}+0.388_{mss4}$	
Yellow stuff	$Y = -0.899_{mss1}+0.428_{mss2}+0.076_{mss3} -0.041_{mss4}$	
Non-such	$N = -0.016_{mss1}+0.131_{mss2}-0.452_{mss3}+0.882_{mss4}$	
	Landsat Thematic Mapper (TM)	Crist, 1985
Brightness	$B = 0.0242_{tm1}+0.4158_{tm2}+0.5524_{tm3}+0.5741_{tm4}+0.3124_{tm5}+0.2303_{tm7}$	
Greenness	$G = -0.1603_{tm1}-0.2819_{tm2}-0.4939_{tm3}+0.794_{tm4}-0.0002_{tm5}-0.1446_{tm7}$	
Wetness	$W = 0.0315_{tm1}+0.2021_{tm2}+0.3102_{tm3}+0.1594_{tm4}-0.6806_{tm5}-0.6109_{tm7}$	
Infrared Index (II)	$II = \frac{NIR_{TM4} - MidIR_{TM5}}{NIR_{TM4} + MidITR_{TM5}}$	Hardisky et al., 1983
Soil Adjusted Vegetation Index (SAVI)	$SAVI = \frac{(1 + L)(NIR - red)}{NIR + red + L}$	Huete, 1988; Huete and Liu, 1994;

Table 2.3 (cont).

Atmospherically Resistant Vegetation Index (ARVI)	$ARVI = \left(\frac{p^*_{nir} - p^*_{rb}}{p^*_{nir} + p^*_{rb}} \right)$	Kaufman and Tanre, 1992; Huete and Liu, 1994
Soil and Atmospherically Resistant Vegetation Index (SARVI)	$SARVI = \frac{p^*_{nir} - p^*_{rb}}{p^*_{nir} + p^*_{rb} + L}$	Huete and Liu, 1994; Running et al., 1994
Enhanced Vegetation Index (EVI)	$EVI = \frac{p^*_{nir} - p^*_{red}}{p^*_{nir} + C_1 p^*_{red} - C_2 p^*_{blue} + L}(1 + L)$	Huete and Justive, 1999

2.4.2 TM Tasseled cap

By analyzing the spectral development of crops over the growing season, Kauth and Thomas (1976) considered the soil spectral as well and recognized that all other four spectral channels data contain useful information. The original conceptual model for this was called "tasseled cap". While statistically rotating the data space into physically meaningful set, Thomas (1976) explored the idea of brightness and greenness. With the launch of Landsat, the model called "TM-Tasseled cap" – a series of indices (brightness, greenness and wetness) was derived.

Brightness and Greenness were reformulated to account for new sensor characteristics, and wetness was designed to contrast the SWIR bands against the visible and NIR bands to express the water content of soils (Crist and Cicone, 1984). The Tasseled Cap transformation is a global vegetation index. It could be used anywhere to disaggregate the

amount of soil brightness, vegetation and moisture content in individual pixel in Landsat MSS and TM image.

2.4.3 Principal component transform

Principal components transformation (PCT) is suggested for efficient hyper-spectral remote-sensing image classification and display. The advantage of using a PCT is that global statistics are used to determine the transformation parameters. The multispectral nature of remote sensing image data can be contained by constructing a vector space with as many axes as there are spectral components associated with each pixel. With Landsat Thematic Mapper data, it will have six dimensions. The first principal component image will be expected to contain 95% of the data variance. The variance in the last component is seen to be minor and this component will appear almost totally as noise of low amplitude. An application of principal components analysis is in the change detection with time between images of the same region (Richards and Jia, 2006).

2.5 Applications of NDVI

The time series analysis of seasonal NDVI data has provided a method of monitoring phonological patterns of the Earth's vegetated surface. Chang (2007) monitored and mapped corn and soybean in the United States using 500-m MODIS NDVI time series data. Brian and Stephen (2005) used 250-m MODIS NDVI data to build state level crop maps in the US Central Great Plains and demonstrated that time-series MODIS 250m NDVI is a possible option for accurate and detail regional-scale crop mapping in the US Central Great Plains with relatively high accuracies (> 84%). Jianqiang et al., (2006) used MODIS_NDVI data for Shandong, China to estimate regional winter wheat yield.

Landsat TM/ATM+ data with multiple spectral bands and 30 m resolution have proven useful for watershed–scale crop mapping (Van Niel et al., 2005; Mosiman, 2003). The LULC maps derived from Landsat TM and ETM+ data, such as United States Geological Survey's (USGS) National Land Cover Dataset (NLCD) (Homer et al., 2004) and Gap Analysis Program (GAP) datasets (Wardlow et al., 2006) have classified cropland area into a single or limited number of thematic classes and are infrequently updated. The United State Department of Agriculture (USDA) National Agricultural Statistic Service (NASS) 30 m crop land data layer (CDL) is detailed and annually updated (Craig 2001). However, the production of LULC datasets from CDL in previous years was limited to a number of selected portions of the US and the methodology to create CDL maps of NASS based solely on their detailed annual sampling data are not available outside the agency. Landsat TM/ETM+ data for local land cover classification has been demonstrated (Collingwood, 2008). However, data availability and quality issues (cloud cover) associated with acquiring imagery at optimal times (growing season) are a factor (DeFries and Belward, 2000) due to their limited temporal resolution. Coarse resolution, time series MODIS NDVI data are useful for land cover classification for regional/national scale up to the global scale (Wardlow et al., 2007; Zhang et al., 2003). The method used in this research was unsupervised classification of multiple Landsat TM images and identified classes based on MODIS-derived NDVI trends for selected crop types in the watershed area, including winter wheat (winter crop), corn, soybean, grain sorghum (summer crops) and grassland - both hay and pasture to support beef cattle production and as Conservation Reserve Program (Lerch et al., 2008)

Based on NDVI values over a growing season in NDVI-time coordination, a crop growth dynamic useful for the classifying process was achieved. This profile shows the variation of NDVI of crop from plant to harvest. Each crop type has a unique, well defined multi-temporal NDVI profile. These profiles should reflect unique phenological characteristics of crop types.

2.6 GIS and Remote Sensing Software

A geographic information system (GIS) is a set of tools used to capture, store, analyze, manage, and present data that are linked to locations. GIS can be used as a merging of cartography, statistical analysis and database technology. Remote Sensing software is Image Processing software for reading, processing, analyzing and displaying information from digital geospatial imagery.

There are several GIS and Remote Sensing software used nowadays. In this study, three programs were used: ERDAS IMAGINE 9.1, ENVI 4.7 and ArcGIS 9.3. ERDAS IMAGINE was used most in this study to treat and analyze Landsat data. Model maker tool in ERDAS was used to integrate raster spatial analysis and design new image processing techniques. Unsupervised and IMAGINE Expert Classifier were used to build and perform geographic expert system for image classification and post classification.

ENVI was used most of the time with MODIS NDVI data and to assess and analyze MODIS NDVI profile for each type of crops. Also the SPEAR tool in ENVI was useful to link between observed areas with Google Earth Image, which is a good source for Geocorrection and Geo reference. ArcGIS was used to build the research area boundary from

NASS county boundary and to build sample points from field data to use in accuracy assessment process.

Chapter 3

METHODOLOGY

3.1 Study site

The Salt River basin (Figure 3.1) is located in northeastern Missouri. River and stream flow from the Upper Salt River drains into Mark Twain Lake since the closing of Clarence Cannon Dam in 1983. Mark Twain Lake, a 7533 hectare reservoir with a shoreline of 460 kilometers, is the source of drinking water for approximately 42,000 people in the area. About 6000 km^2 of total watershed area drains into the four streams: the North Fork (26%), South Fork (14%), Middle Fork (14%) and Elk Fork (12%) (Allen, 2000). The other five sub-basins in the area are Long Branch (8%), Lick Creek (6%), Crooked Creek (5%), Otter Creek (5%), Black Creek and several small streams (10%). The South Fork sub-basin, which begins in Audrain and Boone counties, and the Lick Fork sub-basin, which begins in Audrain, drain northward to Mark Twain Lake. Elk Fork begins in Randolph and drains eastward to Mark Twain Lake. Both the Middle Fork, which begins at Adair-Macon county, and the North Fork, which begins at Schuyler county, drain southeastward to Mark Twain Lake. Two major soils in the drainage area are the Putman-Mexico and Mexico-Leonard-Armstrong-Lindley (SCS 1974-Ralls county; 1979-Knox, Monroe and Shelby counties, 1989-Randolph County), both which are characterized by moderate to high clay content. Landform is classified as: 16 percent upland (0-3 percent gradient); 45 percent gentle slopes (3-10 percent gradient); 21 percent steep slopes (>10 percent gradient) and 18 percent floodplains (0-3 percent gradient). Only the areas near streams and river, and steeply sloping sites were originally forested. Agriculture accounts for 77 percent of land in the basin (Lerch et al., 2008). Land cover types of five major sub-basins in the watershed are given in Table

3.1. Corn, soybean and wheat are the predominant crops grown in the basin (SCS 1974, 1979, 1989). Characterized by clay pan soils, which are especially susceptible to soil erosion, and gentle slope, the watershed results in a high runoff potential. Finney (1986) estimated that 95 percent of sediment supplied to Mark Twain Lake would be trapped in the reservoir. Suspended matter deposited in reservoirs reduces their storage capacity and their ability to control flooding (Choubey and Subramanian, 1992). Sediment affects water quality and its sustainability for drinking water, recreational and industrial uses (Lodhi et al., 1997). Because of the documented soil and problems of herbicide and sediment in surface water, water quality and flow monitoring were initiated basin-wide in 2005 and the Salt River basin was selected as one of twelve USDA Agricultural Research Service (ARS) benchmark watersheds for the Conservation Effects Assessment Project (CEAP) (Lerch et al., 2008). Besides monitoring surface runoff flow and sample water quality in streams, a regional land use and geology land classification were required to develop a cropping system to improve watershed management.

Table 3.1 Gradients, basin area and percentages of cover types in the Upper Salt River Basin in 1990 (Skadeland, 1992)

Percent Land Cover Types						
Stream	Area (ha)	Gradient	Crop	Grass	Forest	Other
Major inflows to Mark Twain Lake:						
Lick	24,179	0.18	70	16	12	2
Elk	57,794	0.18	52	25	18	5
South	76,748	0.17	56	21	18	5
Middle	91,421	0.12	41	32	21	6
North	116,397	0.11	51	28	12	9

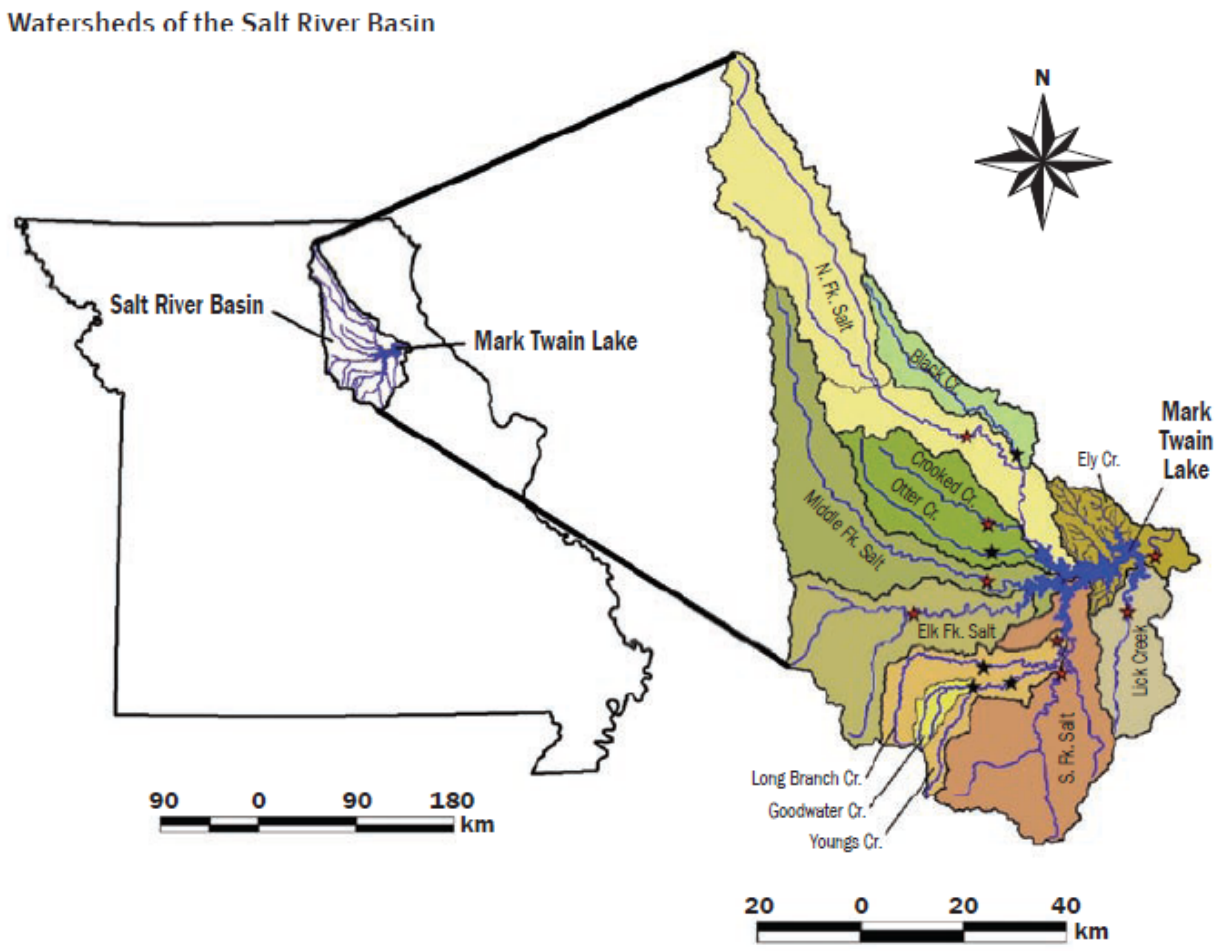

Figure 3.1 Salt River Basin (Lerch et al., 2008)

3.1.1 Summer crops

Summer crops planted in the area are corn, soybean and grain sorghum. Although these summer crops have similar crop calendars, each has a unique spectral-temporal response and different appear among crops. Summer crops have their growth cycles occur during summer, with mid-summer peak NDVI values (peak greenness). The timing and amount of rainfall and the heat and dryness are two weather factors that affect summer crop growth stage and greenness. The USDA NASS has the information about initial planting date for corn, soybean, and sorghum for Missouri.

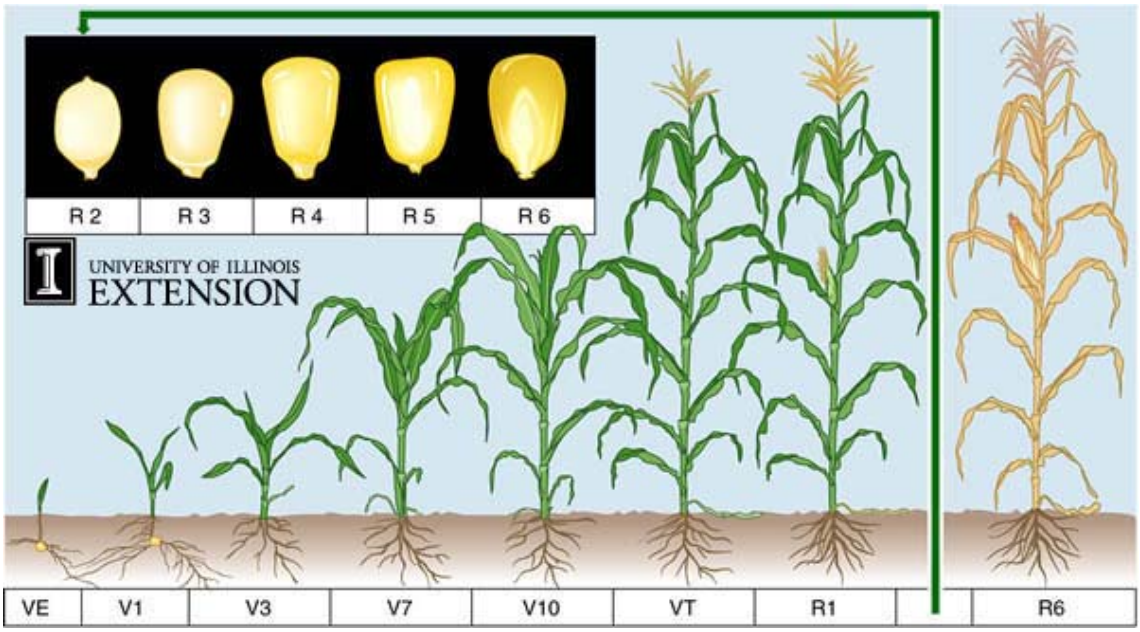

Figure 3.2 Corn Growth Stage Development (Source: http://weedsoft.unl.edu/documents/GrowthStagesModule/Corn/Corn.html#)

Corn growth stage is shown in Figure 3.2. Corn is planted after snow is gone and the soil is thawed. Typical corn plants develop 20-21 total leaves, silk about 65 days after emergence and mature around 125 days after emergence. Corn is the earliest planted summer crop (initial planting date is mid-April and to early June). Corn had the earliest green up, between June 10 and June 26. Corn NDVI peaked in the watershed area during the August 13 period with the NDVI value about 0.77 and higher (Wardlow et al., 2007). Mid-September until mid-October represents the senescence phase of corn, which shows the large NDVI decrease on the NDVI profile.

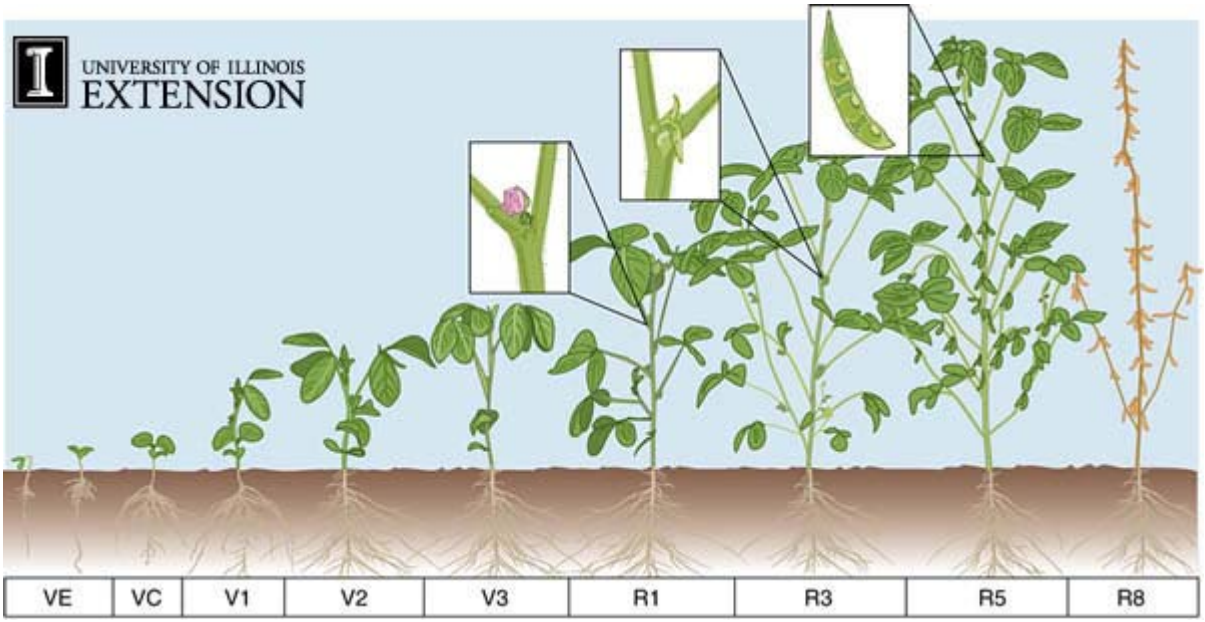

Figure 3.3 Soybean Growth Stage Development (Source: http://weedsoft.unl.edu/documents/GrowthStagesModule/Soybean/Soy.html#)

Soybean Growth Stage is shown in Figure 3.3. Soybean has a wide range of planting dates, but is typically after corn. May 1 to Jun 10 is the normal period to plant soybean. Planting later in June could result in a loss of soybean yield. Double crop (soybean planted after harvesting small grain) in northern Missouri may result in failure because of a shorter growing season (Harry and William, 1949). Double cropping in the Salt River basin area is more successful when there is sufficient soil moisture immediately after the small grain harvest. Soybean green up period is about July 12. Peak greenness of soybean is around August 29 with an NDVI value about 0.84 and higher (Wardlow et al., 2007). Soybean maintains a high NDVI until late-September and has a rapid NDVI decrease in mid-October, representing the senescence phase of soybean (Rogers, 1997).

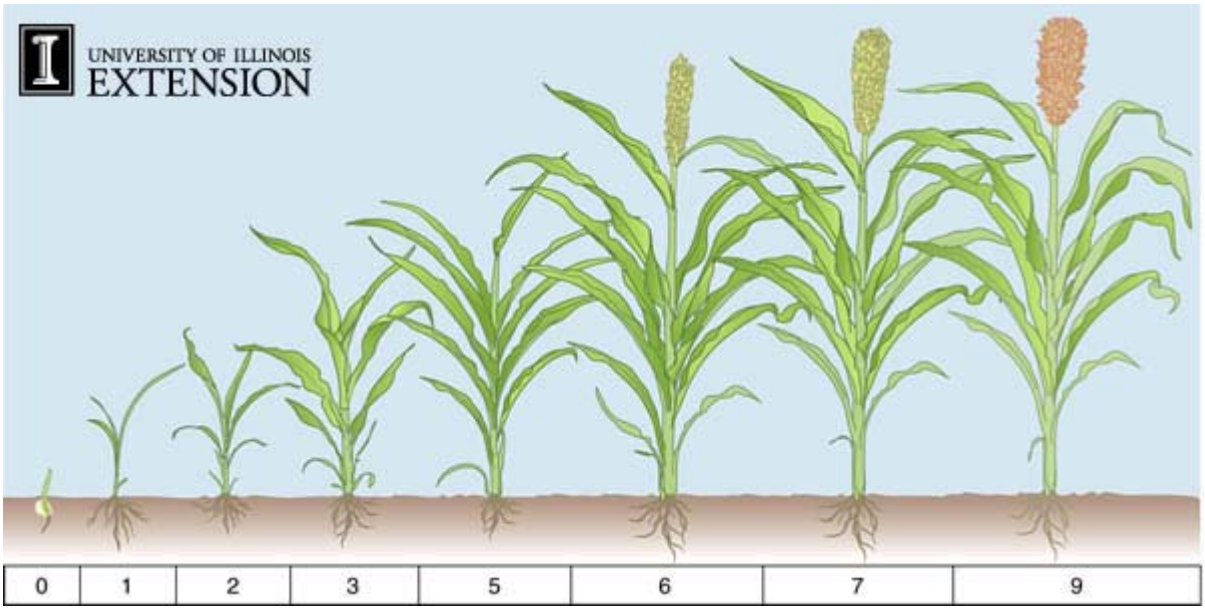

Figure 3.4 Grain Sorghum Growth Stage Development (Source: http://weedsoft.unl.edu/documents/GrowthStagesModule/Sorghum/Sorg.html#)

Grain Sorghum represented about 4 to 6 % of the cropped area in six counties of the study area (based on USDA NASS county-level crop statistics for 2005 and 2006). Grain sorghum growth stage is shown in Figure 3.4. Most grain sorghum was planted in Audrain county and some sorghum fields in Boone, Callaway, Monroe, Ralls and Shelby counties. Initial planting dates for grain sorghum were April 21 and planting continued until early June. Grain sorghum experiences rapid growth beginning 30 days after emergence (between July 12 and July 28). Sorghum peaked greenness during the August 2 period - the same period as soybean but had a lower NDVI value (less than 0.8). Sorghum exhibited a gradual NDVI decrease over a 2-month period, which reflects the extended period for sorghum to dry (Vanderlip et al., 1998)

3.1.2 Winter crops

Wheat is a cool season crop that grows at temperatures as low as 37 degree F. In Missouri, the growing season of winter wheat is from mid-October (plant) till June (harvest)

of the next year. There are three highlight points on the winter wheat NDVI profile. Start-up point begins with low NDVI from January through April. Winter wheat greens up rapidly from mid-April. Since other crops are just germinating, it is easy to distinguish winter wheat from the other grains. Peak point occurs in late May until early June, followed by the rapid decrease of NDVI due to wheat's senescence and harvest. Then "valley" point appears after wheat harvests, followed by a second peak resulting from grass and weeds or soybean (if the condition was possible for double cropping). Wheat growth stage is shown in Figure 3.5.

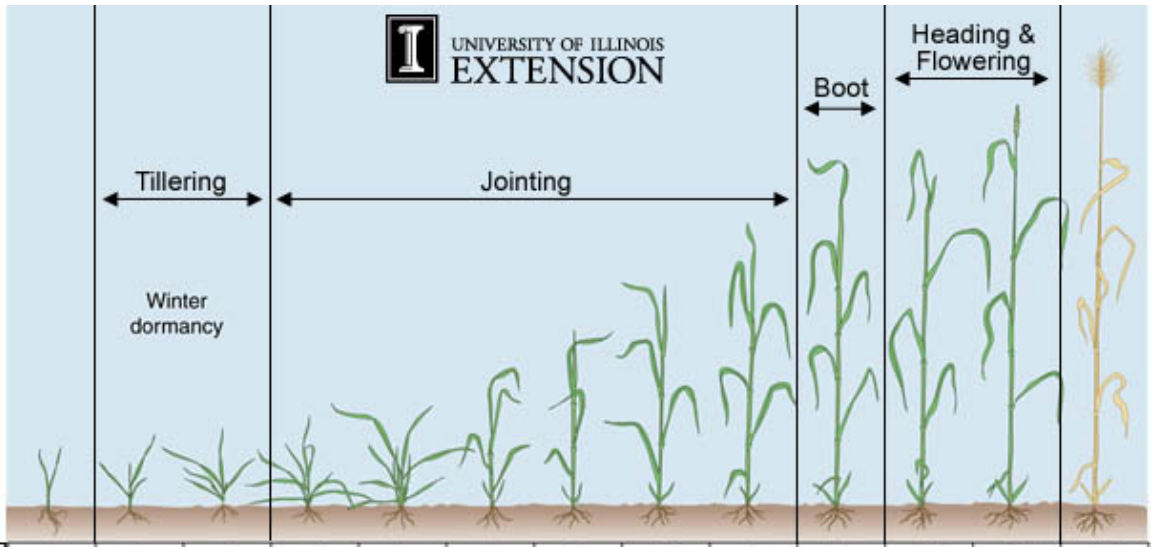

Feekes	1	2	3	4	5	6	7	8	9	10	10.1	10.5	11
Zadoks	10	21	26	30	30	31	32	37	39	45	50	60	90

Figure 3.5 Winter Wheat Growth Stage Development (Source: htttp://weedsoft.unl.edu/documents/GowthStagesModule/Wheat/Wheat.html#)

3.1.3 Grass/Pasture hay

Grass/Pasture hay NDVI profile has a characteristic of grass' phenology of "growth and cut" cycle. Grass/pasture hay begins growth in mid April, represented by a rapid NDVI increase from 0.38 to greater than 0.7. After that, grass, which used as hay, was followed by two or three times of decreasing (cut) and increasing (growth) of NDVI during the summer.

The gradual decrease of NDVI from late October until December matches the senescence of grass/hay.

3.1.4 Other features

Fallow is the practice of leaving the idle field as a dry-land farming technique to conserve soil moisture for the following year (Havlin et al., 1995) resulting in a low NDVI during growing season. Full year fallow is not applied in wet region as Missouri. Short time fallow is applied in several months after wheat is harvested.

Forest, which has high NDVI during the summer, can be separated from cropland by rapid NDVI increase in early summer, remaining high until mid-October with a gradual decrease of NDVI. Water has low NDVI during the entire year, with a slightly NDVI increase in summer due to turbidity of the water body. Urban/developing areas have a low NDVI value and remain almost the same throughout the year.

3.2 Materials

Landsat Thematic Mapper (TM) images for the growing seasons in year 2005 and 2006 were obtained. Due to lack of cloud free imagery, there were only four images for 2005: May 23, June 24, July 10 and Oct 14 and three images for 2006: Apr 8, Sep 15 and Oct 01. A complete image for the study area was created by mosaic Landsat Row 32 Path 25 and Landsat Row 33 Path 25 (Figure 3.6). The complete image from Landsat TM was a layer stack of 6 bands. Landsat TM images were at level 1 geometrically corrected, meaning that it was provided systematic radiometric and geometric accuracy. The scene had been rotated, aligned, and georeferenced to UTM map projection.

The 16-day composite 250m resolution MODIS Terra NDVI product was acquired through NASA-DAAC EROS Data Center. The upper part of the watershed area was in h10v4, which was in zone 13 and the lower part of the watershed was located in h10v5, which was in zone 15. There were three kinds of errors associated with MODIS data product beside cloud cover – geo-referencing, atmospheric correction and bidirectional reflectance distribution function (BRDF) effect. Errors in reflectance are partly reduced with NDVI. In order to reduce this effect, Doraiswamy et al. (2006) used multiple steps in the Savizky-Golay filtering method to smooth every pixel's time series profile through the entire year.

The area of interest (AOI) used to subset the study from remote sensing data is the county-boundary of 11 counties where the Salt River basin is located (Figure 3.6 and 3.7) The county boundary is available on CARES - Center for Agriculture, Research and Environmental Studies. The Farm Facts in Missouri reported by USDA NASS for 2005 and 2006 was obtained to analyze relationship between weather and crops NDVI.

3.2.1 Reference data

Ground truth data were obtained from USDA NASS CDL map for Missouri in year 2006 (Figure 3.8). Reference data were also collected from field observations in year 2005 and 2006 at two reference areas: Goodwater Creek and Greenley, MO. These two data sets were used for accuracy assessment of 2 maps. Results were also compared to county-level crop statistics (USDA NASS) (Table 3.2 through 3.4).

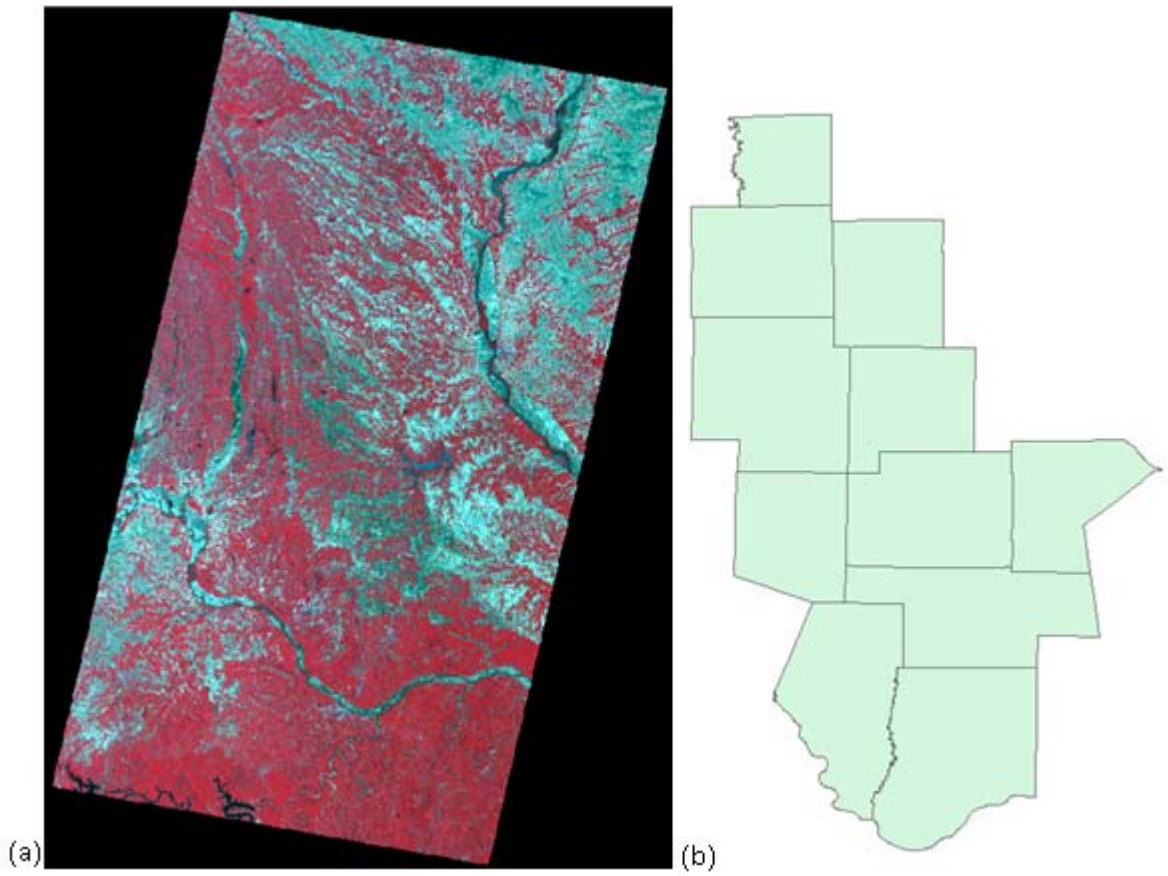

Figure 3.6 (a) A mosaic of Landsat TM row 32 and 33 path 25 (23 May 2005) and (b) Salt River Basin county-boundary.

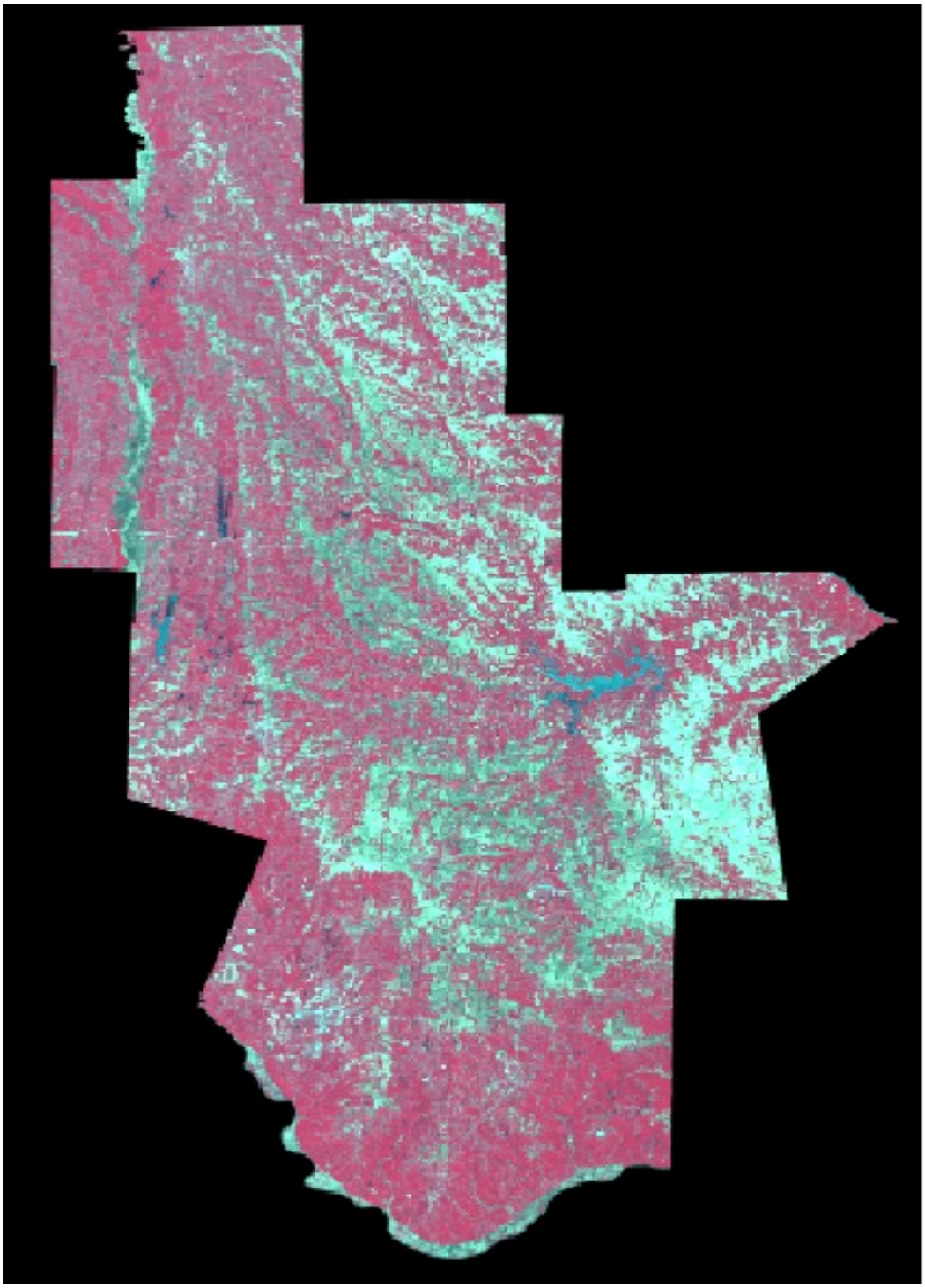

Figure 3.7 False color Landsat image for 23 May 2005 subset to the county boundary of Salt River Basin.

Table 3.2 USDA NASS county statistics (2000)

	Water (mi^2)	Land (mi^2)	Total (acres)
Adair	2.313	567.005	362883.2
Audrain	3.692	693.096	443581.4
Boone	5.881	685.43	438675.2
Callaway	8.194	838.836	536855
Knox	1.067	505.774	323652.5
Macon	8.762	803.769	514412.2
Monroe	24.244	645.982	413428.5
Ralls	12.819	470.998	301438.7
Randolph	5.331	482.319	308684.2
Schuyler	0.288	307.868	197035.5
Shelby	1.495	500.935	320598.4
Total (11 counties)	74.086	6502.012	4161245

Table 3.3 USDA NASS county-level crop statistics for 2005 (acres)

	Corn harvested	Sorghum harvested	Soybean harvested	Wheat harvested	Hay harvested
Adair	14000	x	38800	1400	50000
Audrain	72100	20000	157400	11400	24000
Boone	24100	3600	43500	4300	37000
Callaway	19800	4000	59400	6600	46000
Knox	40200	x	75800	1600	27000
Macon	24700	x	73000	6000	54000
Monroe	48300	4700	74600	2900	31000
Ralls	46800	3900	74700	6600	18000
Randolph	15300	1100	44100	4400	35000
Schuyler	8500	x	18200	x	29000
Shelby	42800	4100	93500	6100	25000

Table 3.4 USDA NASS county-level crop statistics for 2006 (acres)

	Corn harvested	Sorghum harvested	Soybean harvested	Wheat harvested	Hay harvested
Adair	11900	x	38200	3700	51000
Audrain	67200	15000	168000	24400	26000
Boone	19300	2500	46300	9500	38000
Callaway	19500	3500	61500	10400	53000
Knox	34800	x	71700	7600	27000
Macon	20400	x	75200	10700	49000
Monroe	42600	3000	77300	12800	34000
Ralls	42700	2500	79500	14200	21000
Randolph	13800	x	43000	9500	40000
Schuyler	6400	x	18500	900	29000
Shelby	37700	3400	98400	11500	29000

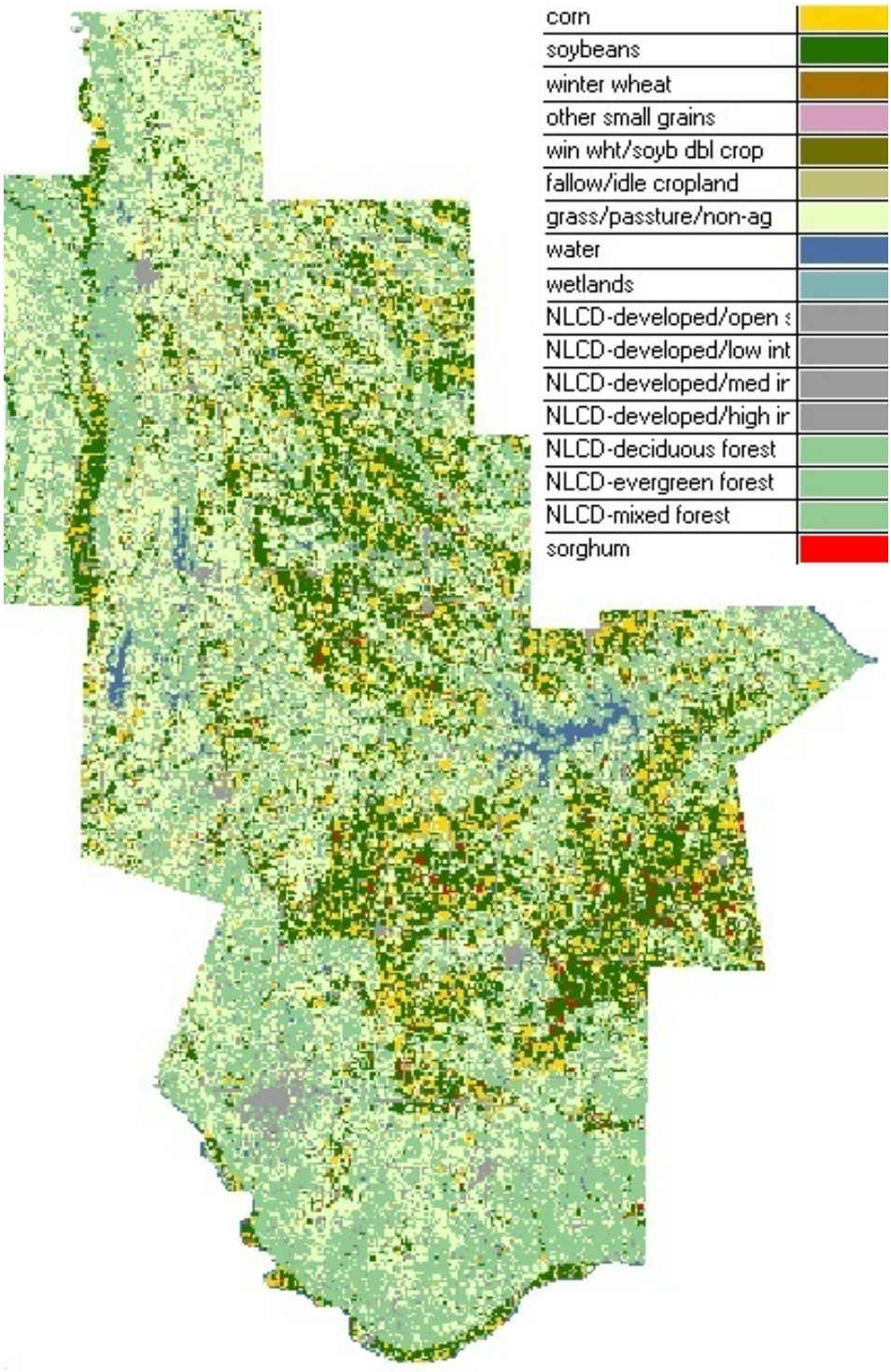

Figure 3.8 USDA NASS CDL map subset to the Salt River Basin (2006).

3.3 Image Preprocessing

The coordinate of Landsat images were adjusted to match the mosaic USGS DOQQ image (from CARES) for the study area. The images after adjustment were also checked with Google Earth using the SPEAR application in ENVI at points as intersection of highway on image.

Song et al. (2001) stated that no atmospheric correction is required if the classification was done based on multiple date composite imagery composited if all of them were rectified and in a single dataset. Kawata et al. (1990) also stated that atmospheric correction has little effect on classification accuracy, as long as the training data and the image are on the same relative scale. Since in this study, the author used all the images used for classification from Landsat 5 TM for multiple dates at the same place, no the atmospheric correction was applied.

A NDVI image derived from Landsat TM data band 3 (Red) and band 4 (near IR) with the equation

$$NDVI = \frac{(Band4 - Band3)}{(Band4 + Band3)} \tag{3.1}$$

NDVI is a unitless index and the NDVI data derived from Landsat TM is expressed in number of ranges -1 to 1.

In addition to 6 bands from Landsat TM and NDVI data derived from Landsat, three other components were used: brightness, greenness and wetness. Tasseled cap values for the Landsat 5 TM were generated using the application in ERDAS Imagine.

The MODIS images (zones 13 and 15) were clipped into smaller portions to re-project to the same zone and then were re-projected from ISIN projection to UTM using ENVI. The ERDAS Imagine was then used to subset the imagery using AOI (area of interest) as the boundary of the eleven counties in the Salt River basin. After that, a twenty-three 16 days 250m NDVI product was built by layer stacking 23 MODIS NDVI images (for a whole year). A small model was built in ERDAS to smooth the NDVI curves for each pixel in the image using a 2nd order polynomial and 7 point Savitzky-Golay filter. The equation for this particular Savitzky-Golay smoothing is defined as follows:

$$y_t = \frac{\left(-2x_{t-3} + 3x_{t-2} + 6x_{t-1} + 7x_t + 6x_{t+1} + 3x_{t+2} - 2x_{t+3}\right)}{21} \tag{3.2}$$

Figure 3.9 shows the smoothing results.

3.4 Previous crop discrimination study on the Salt River watershed

Jang et al. (2009) conducted a previous study done on the Salt River watershed to create a crop type classification map for 2003 from five dates in the growing season: 26 May, 5 July, 22 August, 7 September, and 23 September. Jang et al. (2009) evaluated and compared two different crop type classification methods using data from the 2003 crop year. The first method used unsupervised classification of multiple Landsat images, followed by manual class identification using ground survey data. The second method also used unsupervised classification of multiple Landsat images, followed by class identification using MODIS-derived seasonal NDVI trends. Jang et al. (2009) concluded that the second method improved the overall accuracy of the crop type map to 86%, compared with an 83% accuracy from method one. They concluded that method two can provide better results with less training data. In creating the 2003 crop classification map, Jang et al. (2009) resampled 250-

m resolution MODIS images to the 30-m resolution of the Landsat image. They combined five Landsat images to make a 30-band composite image and unsupervised this combined image to 150 clusters. They extracted the pixels in the stack of MODIS NDVI images corresponding to each of the 150 clusters and imported them into SAS. The tree procedure was done in SAS to group the 150 classes based on their mean MODIS-derived NDVI trends.

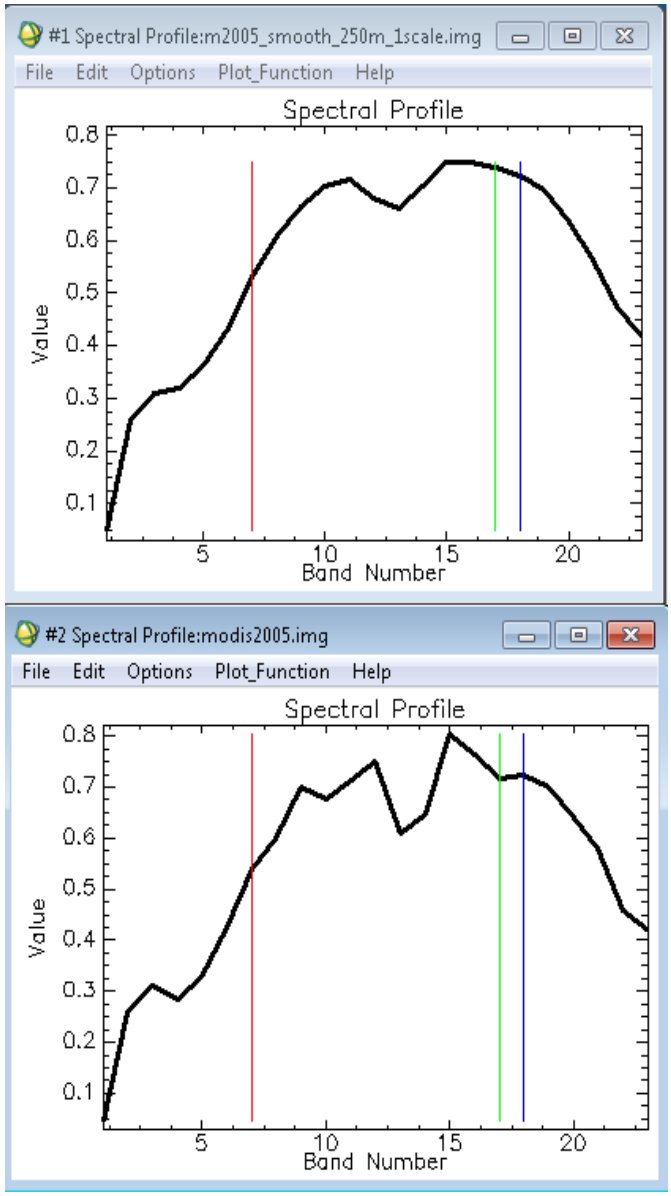

Figure 3.9 The 23-band NDVI trend curve of sample pixel before and after smoothing (extract from ENVI through 2-profile spectral curve).

In this research, the author also used a decision tree and analyzed MODIS-derived NDVI trends to create crop classification maps for the Salt River Basin in 2005 and 2006, but because of the lack of cloud-free Landsat images in the growing season, it was impossible to extract the NDVI trends. In the combination of the three Landsat images in 2006 (April, September and October), trends were similar among summer crops and also similar to grass and forest – with the same green up stage in April and senescence stage in September and October. In the combination of Landsat images in 2005, it would be useful to separate winter wheat and grass from summer crops but there was still a difficulty in discriminate summer crop trends, especially soybean and grain sorghum.

The author chose not to resample 250-m resolution MODIS image because it would provide numerous mixed pixels and be impossible to extract the necessary data such as maximum NDVI, minimum NDVI, date of maximum NDVI, etc. The 23-band MODIS NDVI image was still created to extract the NDVI profile (ENVI z-spectral profile) for each crop type. Crop NDVI profile was then analyzed using the USDA weather report to determine the threshold applied in the decision tree. In this study, the author used unsupervised classification each of Landsat image obtained and create an NDVI map from each Landsat image. The decision tree used in this study was a combination of analyzing pixel NDVI and its possible unsupervised class at each point in time. Principal components transformation and Tasseled cap were also applied in decision tree to get better result.

3.5 Image Processing

In this study, classification was done based on the combination of unsupervised classification (pixel-based) and a decision tree (object-based). The ISODATA method of unsupervised classification was applied using a 0.995 convergence threshold and run with ten

iterations to cluster each Landsat image into 150 clusters. This process was done with ERDAS Imagery. The NDVI profile for each object class in the watershed, such as water, urban, grass, forest, corn, soybean, etc, was examined using ENVI z-spectral profile. Based on the phenological profile of each type, hypotheses were established for creating a decision tree. Unsupervised classification methods have overall good results for agricultural areas (Cohen and Shoshany, 2002), together with object-based methods, which divide the satellite image into objects or segments that represent a homogenous unit on ground, as a way to improve accuracy (Aplin and Atkinson, 2001; Walter, 2004).

3.5.1 Class Identification Process

All 150 clusters from unsupervised classification images were grouped and labeled into nine land cover classes: water, forest, urban, grass/hay, double cropland, winter wheat, corn, soybean and sorghum using ERDAS Imagery using the Knowledge Classifier procedure. All pixels from image were grouped based on its NDVI value for each point of time, spectral characteristics (USC classes) and brightness, greenness and wetness. Knowledge Engineer, an ERDAS Imagery decision tree procedure, known as expert classification, provides a rules-based approach to image classification, post-classification refinement. It is a hierarchy of rules, or decision tree. A rule is a conditional statement or list of conditional statements about an object's attributes that determine a hypothesis.

Chapter 4

RESULTS AND DISCUSSION

4.1 Analysis

4.1.1 Analysis of Landsat data in 2006

Landsat 2006 cloud free data were obtained April 8, September 15 and October 01 , which are shown as red, green and blue lines in MODIS NDVI profiles (Figure 4.1 to 4.6). From the Weather Review Report from NASS for Missouri in year 2006, wet March followed by dry April pushed wheat maturation ahead of normal. Wheat NDVI values had not yet reached the peak greenness in April but were high and close to peak in late May with NDVI value greater than 0.6 (Figure 4.1). Most of April was dry which allowed rapid planting of row crops, but NDVI values for these summer crops were still low (less than 0.4) (Figure 4.2 to 4.4). Grass and forest were greening up at the time the April Landsat image was obtained, with a NDVI greater than 0.5 but still less than winter wheat (Figure 4.5 and 4.6).

At the time the second and third Landsat images were obtained on September 15 and October 01, the corn harvest was already finished. Heat and drought in the first part of August stressed the pasture and row crops. By August 27, Farm Fact reported that 90% of corn was in the dent stage with harvest to soon follow. In early to mid September, soybean and sorghum were just passed peak greenness and maintained a high NDVI value. Sorghum began senescence with onset of dry weather, while soybean still had a high NDVI value (Figure 4.3 and 4.4). Dry and sunny weather over the first half of October made for a good harvest condition. Soybeans had a rapid NDVI decrease in October but sorghum had a more

gradual decrease in the NDVI curve. The forest area kept a high NDVI value during the observed period (Figure 4.5). Grass had cutting and re-growth NDVI curves (Figure 4.5) but due to cloud cover during much of the satellite sampling periods, the NDVI trends of grass/hay through three points of time had some characteristics similar to soybean and sorghum.

Corn exhibited low NDVI in these three points of time, since in April it was just planted, and by September, it was already in the dent stage and with harvesting completed by the end of September (Figure 4.2). The rapid decrease of NDVI from mid September to early October helped to discriminate soybeans from other crops (Figure 4.3). Mixed pixels appeared at the boundary of fields, which had some characteristics similar to sorghum (gradual drop of NDVI). Therefore, other components were applied to better classify sorghum, soybean and grass/hay. These differences among vegetation types were applied to build the hypotheses in the decision tree.

4.1.2 Analysis of Landsat data in 2005

Landsat 2005 cloud free data were obtained May 23, June 24, July 10 and October 14. May 23, June 24 and July 10 were the three images during the growth season of summer crops. The October 14 image was in late fall, when all summer crops were already in the senescence stages but since there was lack of cloud free images in the growth season to classify between summer crops, it was useful in providing additional information to better discriminate between corn, soybean and grain sorghum.

The Weather Review Report from NASS for Missouri in 2005 indicated that by the end of April, 72% of corn was in the ground but light frost in late April burned the upper

leaves. Wheat was processing well, mostly in fair to good condition. A dry cool May slowed the growth of crops. During the third week of May, corn planting reached 98 percent. By the end of May, 85 % of soybean and 90 % of grain sorghum were planted. The May 23 Landsat image coincided with winter wheat reaching its greatest NDVI value. Grass and forest also had a high NDVI value. Rain in early June improved summer crop growth. The wheat harvest began the second week of June with 83 % of winter wheat harvested by the end of June. The Landsat June 24 image showed the low NDVI condition of winter wheat fields and increased NDVI value of other summer crops. Comparing NDVI values from Landsat images of May 23 and June 24 revealed the information to separate winter wheat from other crops. But extra information was needed to classify winter wheat and hay since hay harvest in June also reduced its NDVI value.

Drought conditions were during mid August and the peak NDVI of soybeans and sorghum were in late August (Figure 4.3 and 4.4). The ideal time to separate classes between summer crops was during August and early September, when corn was harvested, grain sorghum was in senescence but soybean maintained a greater NDVI value. Unfortunately, no cloud-free Landsat image was obtained in that time. In October, a few periods of showers slowed fall harvest. By the end of October, 93 % of corn was out of the field, 83 % of soybean and 86 % of grain sorghum were harvested. Due to the fact that soybean NDVI drops more rapidly than grain sorghum, the October 14 Landsat image was useful in identifying each since soybean had a lower NDVI compared with grain sorghum. Analyzing NDVI differences between July and October also assisted in classifying soybean and grain sorghum.

Besides analyzing the NDVI value of vegetation, the information from Principal Components and Tasseled Cap were also valuable in identifying differences over time. For example, in June, when wheat was harvested, the NDVI of wheat was as low as grass. But wheat fields had a greater brightness than grass. Tasseled Cap brightness was used to classify urban/soil/fallow from vegetation. Tasseled Cap wetness was used to better separate water bodies and wetland from other features.

4.1.3 Crop NDVI profiles

Crop NDVI profiles were obtained from MODIS 2006 data in Salt River Basin watershed. The red line (left vertical line Fig. 4.1 to 4.6) is at the 7th band, the blue line (right vertical line) is at the 18th band and the green line (middle vertical line) is at the 17th band in a 23-day MODIS NDVI trend curve. The combination of these three bands (bands 7, 17 and 18) as red, green, blue match with the combination of three Landsat NDVI images obtained in 2006.

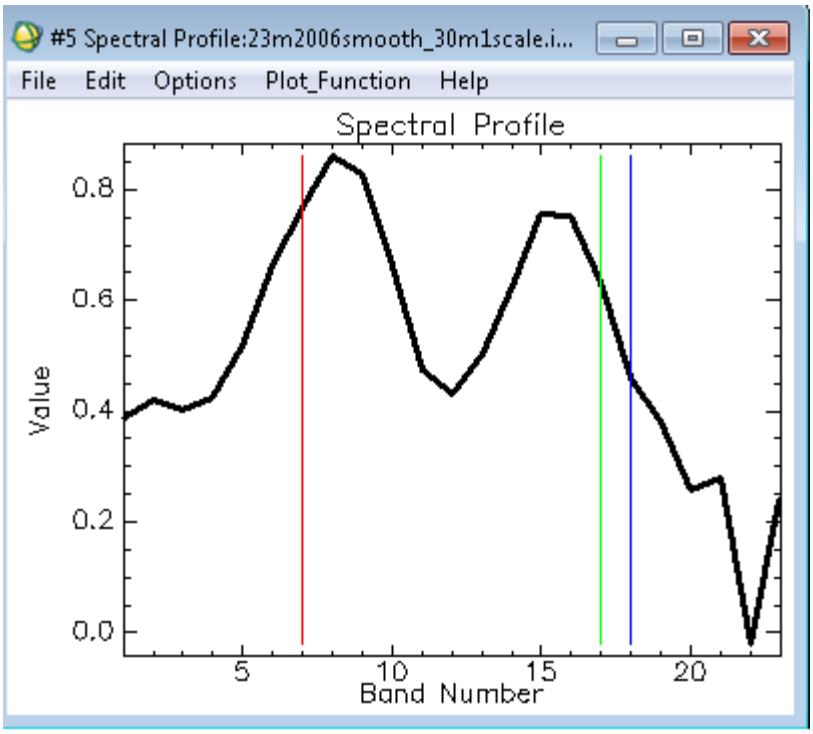

Figure 4.1 MODIS Winter Wheat NDVI profile in 2006.

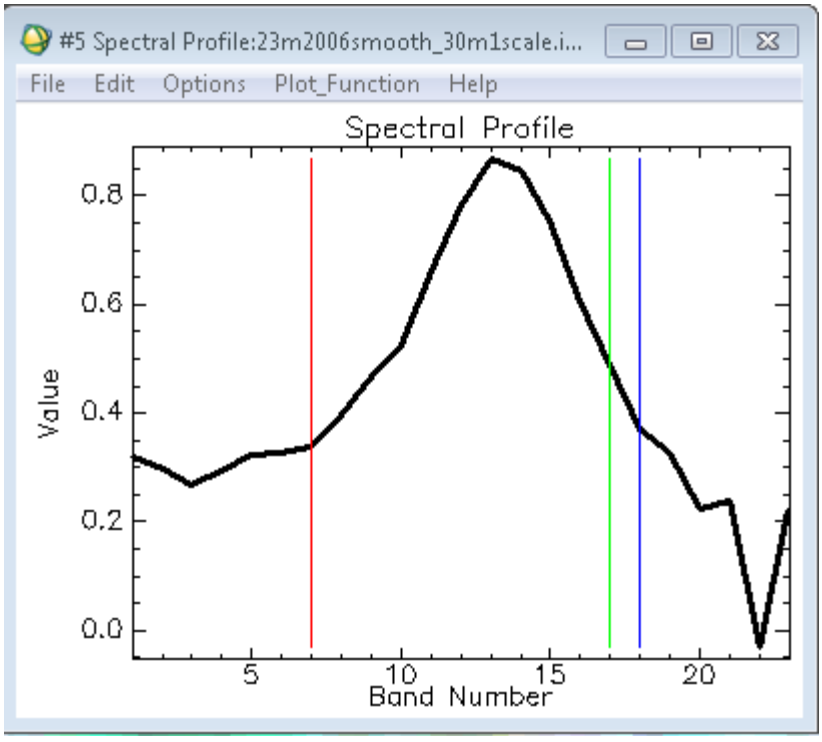

Figure 4.2 MODIS Corn NDVI profile in 2006.

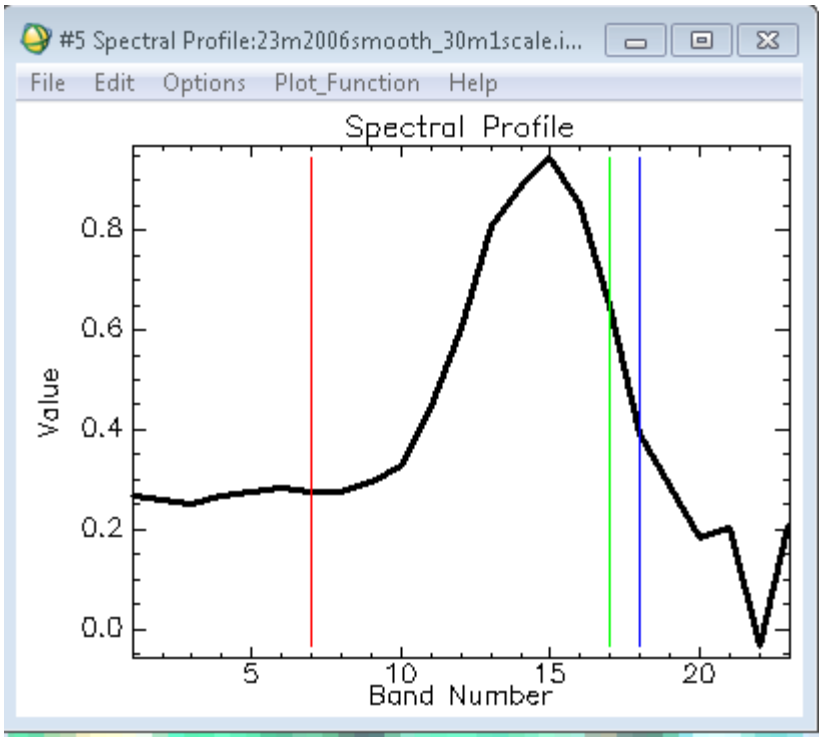

Figure 4.3 MODIS Soybean NDVI profile in 2006.

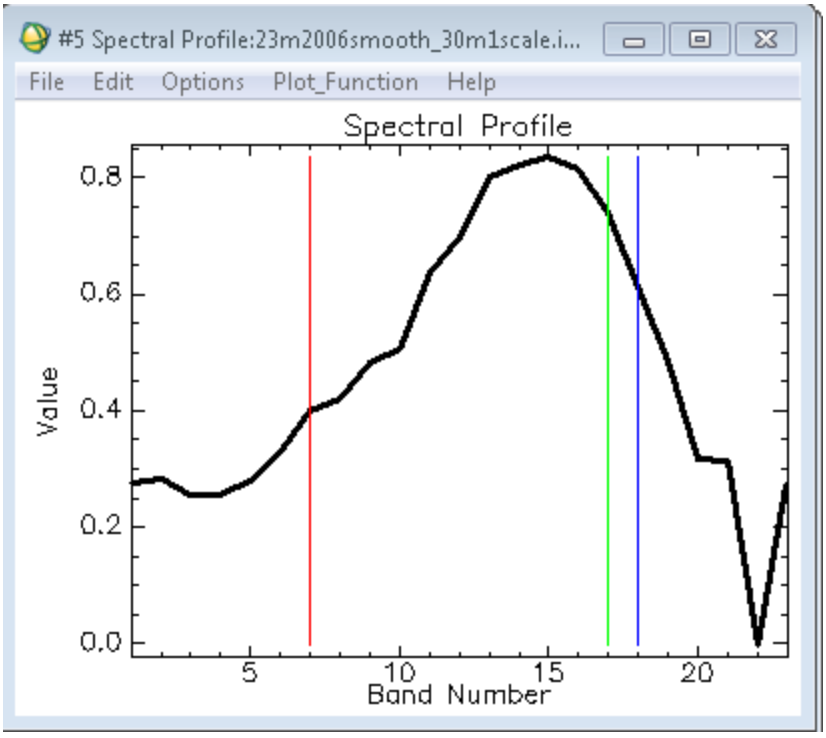

Figure 4.4 MODIS Sorghum NDVI profile in 2006.

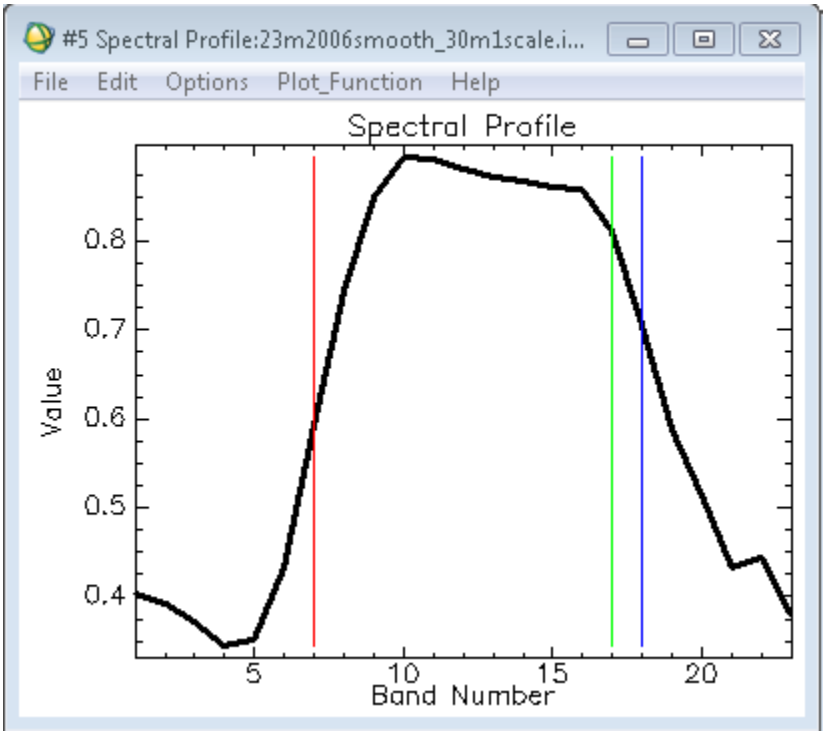

Figure 4.5 MODIS Forest NDVI profile in 2006.

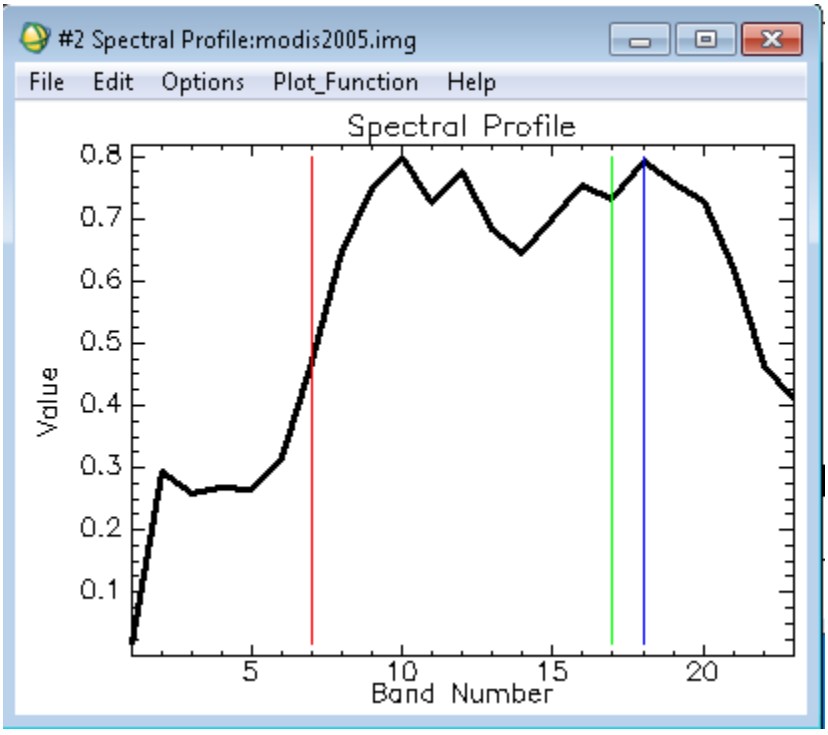

Figure 4.6 MODIS Grass NDVI profile in 2006.

4.2 Decision tree rules

The decision tree was built using the Knowledge Engineer Module in Erdas Imagine. This program provides a graphical user interface for the "expert" to build a tree diagram consisting of final and intermediate class definitions (hypotheses), rules (conditional statements concerning variables), and variables (raster, vector, or scalar). Hypotheses are evaluated by the use of rules – if one or more rules are correct, then that hypothesis may be true at that particular location. The rule is evaluated based on input variables in order to determine if a rule is true. Variables could be in the form of an existing image or it could even be an external program. Variables can also be defined from vectors and scalars. If the variable's value indicates that the rule is correct and all the rules defined the hypothesis is correct, the hypothesis (class allocation) is true. Decision trees are shown in Appendix A.

4.2.1 Decision rules to separate water and urban/soil from the others

Both water and urban/soil have a low NDVI value at any point of time, but water bodies show as a black feature in the Landsat image while urban/soil has a bright color in the Landsat image. Applying this analysis, pixels of water would have a low NDVI and USC class less than 20 (black feature), while pixels of urban/soil would be low in NDVI and USC greater than 20.

Soil/fallow pixels would be classified as urban/soil if the area was limited to weeds, but it would be classified as grass if there was an abundance of weeds in idle cropland. Figure 4.7 is as example of decision tree diagram to classify water.

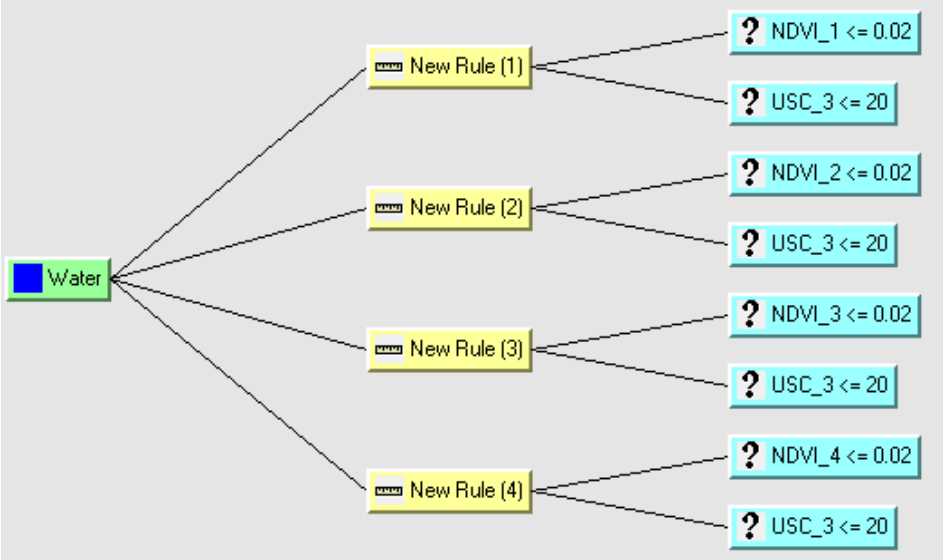

Figure 4.7 Decision rules to define water for 2005

where

- Testing hypothesis: Water
- NDVI_1, NDVI_2, NDVI_3, NDVI_4: NDVI value extracted from Landsat NDVI 2005 images for May 23, June 24, July 10 and October 14 respectively.
- USC_3: unsupervised classification cluster of Landsat TM for June 24, 2005

Explanation of decision tree process for water identification:

If (NDVI_1 ≤ 0.02 and USC_3 ≤ 20) or
(NDVI_2 ≤ 0.02 and USC_3 ≤ 20) or
(NDVI_3 ≤ 0.02 and USC_3 ≤ 20) or
(NDVI_4 ≤ 0.02 and USC_3 ≤ 20)
Then (Water = true)
End if.

4.2.2 Decision rules to separate winter wheat and double crop from the other land uses

Winter wheat has a higher NDVI than other objects in April and May. Winter wheat NDVI could reach 0.45 in April and higher in May (>0.5) while summer crop NDVI remains low. Grass has the same green up stage in April and May, which has an NDVI of 0.45 or greater. Wheat could be separated from grass if there were data in June and July, which

indicates the cutting and regrowth of grass/hay. Winter wheat – fallow shows high NDVI in April and May (>0.5) but low NDVI in September and October (<0.4), which could partly separate it from grass if grass shows the regrowth stage in September and October. Winter wheat – soybean double crop exhibits a high NDVI value in April/May and a high NDVI value in July/August as well. Again, double crop could be mis-classified as grass and vice verse because they exhibit the same trends in April and September.

4.2.3 Decision rules to separate corn from the other summer crops

Corn was the earliest planted summer crop, so its NDVI in April was higher than the other summer crops but less than grass and winter wheat. Corn has the highest NDVI value among summer crops in July (since there was no August image obtained in 2005 and 2006) with a NDVI value higher than 0.5 into September. Some corn was already harvested, and exhibited a bare soil (bright feature) with USC in September greater than 145. Other corn fields that had not yet been harvested had a low NDVI value similar to other summer crops, but the corn harvest was done in late October, with USC in October greater than 130.

4.2.4 Decision rules to separate soybean and grain sorghum

These two summer crops are difficult to separate because they have the same initial planting date and show the same trends during the growing season. During the growing season, soybean always has a higher NDVI value than grain sorghum. The phenology of these two crops in the senescence stage was applied. Soybean NDVI decreases rapidly while grain sorghum has a gradual NDVI decrease. It was possible that grain sorghum NDVI in July was less than the NDVI in September (NDVIJul – NDVISep < 0) due to high air temperature in July and rainfall in August. If NDVI difference from September to October was greater than 0.3, it would be classified as soybean. In 2006, some sorghum pixels had an

NDVI trend similar to grass/fallow, making it difficult to separate grass/fallow from sorghum.

4.3 Accuracy assessment

One of the most common means to express accuracy of classification is the preparation of a classification error matrix. An error matrix is based on category to category comparison, the relationship between known data (reference ground truth data) and results from automated classification. The error matrix expresses omission (exclude) error and commission (include) error. The overall accuracy is also computed by dividing the total number of correctly classified pixels by the total number of reference pixels. In addition, the producer's and user's accuracies are also obtained from the error matrix. The producer's accuracies are the accuracies of individual categories, which are computed by dividing the total number of correctly classified pixels in each category by the total number of pixels in the corresponding column of matrix. User's accuracy is calculated by dividing the number of correctly classified pixels in each category by the total number of pixels in corresponding row.

The $\hat{k}$ (k_hat) statistic (Kappa analysis) was also obtained after the accuracy assessment procedure in ERDAS. The $\hat{k}$ is a measure of the difference between the actual agreement between reference data and an automated classifier and the chance agreement between the reference data and a random classifier. The $\hat{k}$ statistic is computed as (Jensen, 2000)

$$\hat{k} = \frac{N\sum_{i=1}^{r} x_{ii} - \sum_{i=1}^{r}\left(x_{i+} \times x_{+i}\right)}{N^2 - \sum_{i=1}^{r}\left(x_{i+} \times x_{+i}\right)} \qquad (4.1)$$

where

r = number of rows in the error matrix

x_{ii} = number of observations in row i and column i (on the major diagonal)

x_{i+} = total of observations in row i (shown as marginal total of right sideof the matrix)

x_{+i} = total of observations in column i (shown as marginal total of bottom of the matrix)

N = total number of observations included in matrix

The overall accuracy only includes the data along the major diagonal and excludes the errors of omission and commission The $\hat{k}$ incorporates the nondiagonal elements of the error matrix as a product of the last row and column.

Congalton (1991) recommended that a minimum of 50 sample points should be obtained in each category. Since sorghum and wheat were planted in fewer fields than corn and soybean, the number of sample points for each crop varied. The NASS CDL crop map subset to watershed area was used for the accuracy assessment process for the 2006 crop map. For the accuracy assessment for the 2005 crop map, an error matrix was prepared for two reference areas (Goodwater creek sub-basin and Greenley reference area) where ground-truth data were available. For the accuracy assessment for the 2006 crop map, an error matrix was also prepared for two reference areas (Goodwater creek sub-basin and Greenley reference area) where ground-truth data were available. Also, an error matrix was prepared for the whole watershed area for comparison with NASS CDL map.

There were 308 points taken from 141 fields in the Goodwater creek sub-basin and 257 points taken from 168 fields in the Greenley reference area for accuracy assessment process for the 2005 crop map. With the accuracy assessment process for the 2006 crop map, 488 points were taken from 224 fields in Goodwater creek sub-basin and 232 points were taken from 198 fields in Greenley reference area. Sample points were chosen randomly using 2 or 3 points in small fields and more points in larger fields instead of one point per field in order to reduce the chance of taking mixed pixel points.

For the 2006 crop map, the overall accuracy was 87.09% for Goodwater Creek sub-basin (Table 4.4) and 96.98% for Greenley reference area (Table 4.3) compared with field data in two areas, and overall accuracy for the whole watershed area was 94.08% when compared with the NASS CDL map (Table 4.5). The accuracy of Goodwater Creek sub-basin was lower than the Greenley reference area due to the fact that no grain sorghum was planted in the northern part of the basin area. Due to the difference in resolution from the study's map (30 m resolution in Landsat image) and the CDL map (56 m resolution), there were some pixels that were classified in different classes. For example, there were some small ponds inside the urban area that could not be seen in the CDL 56 m resolution but were identifiable with 30 m Landsat resolution. The CDL map was created based on NASS annual survey data that can help to classify more classes than the map from this study, such as grass, hay/pasture, red clover, alfalfa, and etc; and better classify grain sorghum with other crops.

There was no NASS CDL map to use for verifying the 2005 crop map. Accuracy assessment was done with field data taken from the two reference areas in the area. The overall accuracy was 92.53% for the Goodwater Creek sub-basin (Table 4.2) and 93% for the Greenley reference area (Table 4.1). Again, the appearance of grain sorghum in the south

part of the area reduced the overall accuracy of the Goodwater creek sub-basin compared to the Greenley reference area. The accuracy was higher in 2005 compared with the 2006 map since more images were available during the growth season in 2005.

The Kappa coefficient for each accuracy assessment procedure was shown in Table 4.1 through 4.5. Additional statistical comparisons of both crop maps with crop area statistics from NASS were done. Results are shown in Table 4.6 and 4.7

Table 4.1. Accuracy assessment resulting from classifying the crop map in 2005 for the Greenley reference area

ERROR MATRIX

		Reference Data						
		Water	Grass	Winter Wheat	Corn	Soybean	Sorghum	Row total
Classified Data	Water	0	0	0	0	0	0	0
	Grass	0	38	0	0	0	0	38
	Winter wheat	0	3	16	0	0	0	19
	Corn	0	0	0	80	10	0	90
	Soybean	0	1	1	2	105	0	109
	Sorghum	0	0	0	1	0	0	1
	Column total	0	42	17	83	115	0	257

ACCURACY TOTALS

Class name	Reference totals	Classified Total	Number Correct	Producers Accuracy (%)	Users Accuracy (%)
Water	0	0	0	--	--
Grass	42	38	38	90.48	100.00
Winter wheat	17	19	16	94.12	84.21
Corn	83	90	80	96.39	88.89
Soybean	115	109	105	91.30	96.33
Sorghum	0	1	0	--	--
Totals	257	257	239		

Overall Kappa Statistics = 0.8849

Conditional Kappa for each Category

Overall Classification Accuracy = 93.00%

CONDITIONAL KAPPA FOR EACH CATEGORY

KAPPA (K^) STATISTICS

Class Name	Kappa
Water	0.0000
Grass	1.0000
Winter wheat	0.8310
Corn	0.8365
Soybean	0.9335
Sorghum	0.0000

Table 4.2 Accuracy assessment resulting from classifying the crop map in 2005 for the Goodwater creek sub-basin

ERROR MATRIX

		Reference Data						
		Water	Grass	Winter Wheat	Corn	Soybean	Sorghum	Row total
Classified Data	Water	8	0	0	0	0	0	8
	Grass	0	30	1	0	0	0	31
	Winter wheat	0	2	7	0	1	0	10
	Corn	0	0	0	78	5	0	83
	Soybean	0	0	0	4	136	6	146
	Sorghum	0	2	0	0	2	26	30
	Column total	8	34	8	82	144	32	308

ACCURACY TOTALS

Class name	Reference totals	Classified Total	Number Correct	Producers Accuracy (%)	Users Accuracy (%)
Water	8	8	8	100.00	100.00
Grass	34	31	30	88.23	96.77
Winter wheat	8	10	7	87.50	70.00
Corn	82	83	78	95.12	93.98
Soybean	144	146	136	94.44	93.15
Sorghum	32	30	26	81.25	86.67
Totals	308	308	285		

Overall Classification Accuracy = 92.53%

KAPPA (K^) STATISTICS

Overall Kappa Statistics = 0.8826

CONDITIONAL KAPPA FOR EACH CATEGORY

Class name	Kappa
Water	1.0000
Grass	0.9300
Winter wheat	0.6921
Corn	0.9177
Soybean	0.8721

Table 4.3 Accuracy assessment resulting from classifying the crop map in 2006 for the Greenley reference area

ERROR MATRIX

Classified Data	Water	Urban-Soil	Forest	Grass	Wheat/ Soybean	Wheat	Corn	Soybean	Sorghum	Row Total
Water	1	0	0	0	0	0	0	0	0	1
Urban/Soil	0	0	0	0	1	0	0	0	0	1
Forest	0	0	0	1	0	0	0	0	0	1
Grass	0	0	0	36	1	0	0	0	0	37
Wheat/Soybean	0	0	0	0	0	0	0	1	0	1
Wheat	0	0	0	0	1	3	0	0	0	4
Corn	0	0	0	0	0	0	78	0	0	78
Soybean	0	0	0	2	0	0	0	107	0	109
Sorghum	0	0	0	0	0	0	0	0	0	0
Column Total	1	0	0	39	3	3	78	108	0	232

ACCURACY TOTALS

Class name	Reference totals	Classified Total	Number Correct	Producers Accuracy (%)	Users Accuracy (%)
Water	1	1	1	100.00	100.00
Urban/Soil	0	1	0	--	--
Forest	0	1	0	--	--
Grass	39	37	36	92.31	97.30
Wheat/Soybean	3	1	0	0.00	0.00
Wheat	3	4	3	100.00	75.00
Corn	78	78	78	100.00	100.00
Soybean	108	109	107	99.07	98.17
Sorghum	0	0	0	--	--
Total	232	232	225		

Overall Classification Accuracy = 96. 98%

KAPPA (K^) STATISTICS
Overall Kappa Statistics = 0.9529

CONDITIONAL KAPPA FOR EACH CATEGORY

Water	1.0000
Urban/Soil	0.0000
Forest	0.0000
Grass	0.9675
Wheat/Soybean	-0.0130
Wheat	0.7467
Corn	1.0000
Soybean	0.9657
Grain Sorghum	0.0000

Table 4.4 Accuracy assessment resulting from classifying the crop map in 2006 for the Goodwater creek sub-basin

ERROR MATRIX										
Classified Data	Water	Urban-Soil	Forest	Grass	Wheat/ Soybean	Wheat	Corn	Soybean	Sorghum	Row Total
Water	6	0	0	0	0	0	0	0	0	6
Urban/Soil	0	0	0	0	0	0	0	1	0	1
Forest	0	0	2	0	1	0	0	0	0	3
Grass	0	0	0	65	7	0	1	1	8	82
Wheat/Soybean	0	0	0	1	15	1	0	1	0	18
Wheat	0	0	0	0	0	10	0	0	0	10
Corn	0	0	0	0	0	0	118	2	0	120
Soybean	0	0	0	0	0	0	0	203	14	217
Sorghum	0	0	0	0	0	0	0	2	29	31
Column Total	6	0	2	66	23	11	119	210	51	488

ACCURACY TOTALS					
Class name	Reference totals	Classified Total	Number Correct	Producers Accuracy (%)	Users Accuracy (%)
Water	6	6	6	100.00%	100.00%
Urban/Soil	0	1	0	---	---
Forest	2	3	2	100.00%	66.67%
Grass	66	82	65	98.48%	79.27%
Wheat/Soybean	23	18	15	65.22%	83.33%
Wheat	11	10	10	90.91%	100.00%
Corn	119	120	118	99.16%	98.33%
Soybean	210	217	203	96.67%	93.55%
Sorghum	51	31	29	56.86%	93.55%
Total	488	488	437		

Overall Classification Accuracy = 91.80%
KAPPA (K^) STATISTICS
Overall Kappa Statistics = 0.8857

CONDITIONAL KAPPA FOR EACH CATEGORY	
Water	0.0000
Urban/Soil	0.6653
Forest	0.7603
Grass	0.8251
Wheat/Soybean	1.0000
Wheat	0.9780
Corn	0.8867
Soybean	0.9280
Grain Sorghum	1.0000

Table 4.5 Accuracy assessment resulting from classifying the crop map in 2006 for the Salt River Basin watershed

ERROR MATRIX										
Classified Data	Water	Urban-Soil	Forest	Grass	Wheat/ Soybean	Wheat	Corn	Soybean	Sorghum	Row Total
Water	51	4	1	0	0	0	0	0	0	56
Urban/Soil	0	166	4	5	0	0	0	1	0	176
Forest	0	0	180	5	0	0	2	0	0	187
Grass	0	0	0	188	5	0	0	0	0	193
Wheat/Soybean	0	0	0	9	37	0	0	2	0	48
Wheat	0	0	0	5	0	40	2	0	0	47
Corn	0	0	0	7	0	1	190	2	0	200
Soybean	0	0	2	1	0	0	1	196	0	200
Sorghum	0	0	0	6	0	0	0	2	17	25
Column Total	51	170	187	226	42	41	195	203	17	1132

ACCURACY TOTALS					
Class name	Reference totals	Classified Total	Number Correct	Producers Accuracy (%)	Users Accuracy (%)
Water	51	56	51	100.00%	91.07%
Urban/Soil	170	176	166	97.65%	94.32%
Forest	187	187	180	96.26%	96.26%
Grass	226	193	188	83.19%	97.41%
Wheat/Soybean	42	48	37	88.10%	77.08%
Wheat	41	47	40	97.56%	85.11%
Corn	195	200	190	97.44%	95.00%
Soybean	203	200	196	96.55%	98.00%
Sorghum	17	25	17	100.00%	68.00%
Total	1132	1132	1065		

Overall Classification Accuracy = 94.08%
KAPPA (K^) STATISTICS
Overall Kappa Statistics = 0.9302

CONDITIONAL KAPPA FOR EACH CATEGORY	
Water	0.9065
Urban/Soil	0.9331
Forest	0.9552
Grass	0.9676
Wheat/Soybean	0.7620
Wheat	0.8455
Corn	0.9396
Soybean	0.9756
Grain Sorghum	0.6751

Table 4.6 Crop area comparison between map statistic and NASS crop area statistic in 2005

	Wheat	Corn	Soybean	Sorghum	Grass	total area
NASS (in acres)	51300	356600	753000	41400	-	4161245
% area(NASS)	1.2328	8.56955	18.0956	0.9949	-	
map2005 (in acres)	69521.2	339651	672525	31269.9	1400089	4208400
% area (map2005)	1.65196	8.07079	15.9805	0.74304	33.2689	

Table 4.7 Crop area comparison between map statistic and NASS crop area statistic in 2006

	Wheat	Con	Soybean	Sorghum	Grass	total area
NASS (in acres)	115200	316300	777600	29900	-	4161245
% area(NASS)	2.7684	7.60109	18.6867	0.71854		
map2006 (in acres)	81728	301258	745108	31722	1361077	4210076
% area (map2006)	1.94125	7.15563	17.6982	0.75348	32.329	

The NASS Cropland Data Layer (Mueller et al., 2009) provides land cover classification using two inputs: 56 meter multispectral imagery from Resourcesat-1 AWiFS and groundtruth data from the FSA. The Advance Wide Field Sensor (AWiFS) was launched in October 2003 by Indian Space Research Organization and distributed via commercial U.S. Partner EOTech Inc. The large swath width (740km) with corresponding five date repeat cycle increases the potential to obtain cloud-free in-season satellite images with four spectral bands similar to Landsat (TM bands 2, 3, 4 and 5). Combination of AWiFS data with the available Landsat TM data improves classification accuracies. NASS purchased AWiFS scenes over the continental US for CDL production. June Agricultural Survey (JAS) digitized field boundaries were developed by NASS employees for use in the production of the CDLs. NASS used See5 Decision Tree software to produce CDLs. Data sets derived from Landsat imagery were resampled to match the 56 meter resolution of AWiFS pixel resolution. CDLs took advantage of updated satellite imagery and updated farmer reported ground data in June August, September and October to increase the accuracies for the major corn, soybean and

wheat areas. However, in comparison with field data taken in Goodwater Creek sub-basin, some grain sorghum fields in the area were mis-classified as grass and soybeans in the NASS CDL. There was still a problem to differentiate grain sorghum from other classes even though there were more data in the growing season because NDVI signature of grain sorghum is similar to soybean. Additional techniques are required to correctly classify grain sorghum from other classes.

The method that Jang et al. (2009) applied in a previous study done on the Salt River Basin watershed to create a crop type classification map for 2003 using a decision tree method was based on the statistics NDVI trends. This method would be possible to apply if there were enough data in the growth season to extract crop features such as: maximum NDVI, minimum NDVI, period of having maximum NDVI, time from planting until maximum NDVI, period of senescence and etc. This method is difficult to apply when ground truth data is not available to extract characters of crop NDVI.

The strength of the method used in this research is that it based on analyzing the MODIS NDVI profile and effect of weather factors to find threshold NDVI used in a decision tree model. This method also analyzed the overall appearance of crops in images in different periods of time (blackish and grayish of features in USC images).

4.4 Crop type maps

The final objective of this research was to create crop type maps for Salt River Watershed (see Figure 4.8 and 4.9).

The crop map of 2005 showed a higher accuracy when compared with the crop map of 2006. This emphasizes the value of Landsat data in the growth season for the

discrimination process. However, the idea of obtaining early season and late season data can also help to classify crops from other features, as well as among summer crops. The Farm Fact data (USDA NASS) was very important in understanding and analyzing the NDVI value of each object in the area. The difference in crop area estimation between this and other methods can be explained first by the weather effect and secondly by the image resolution.

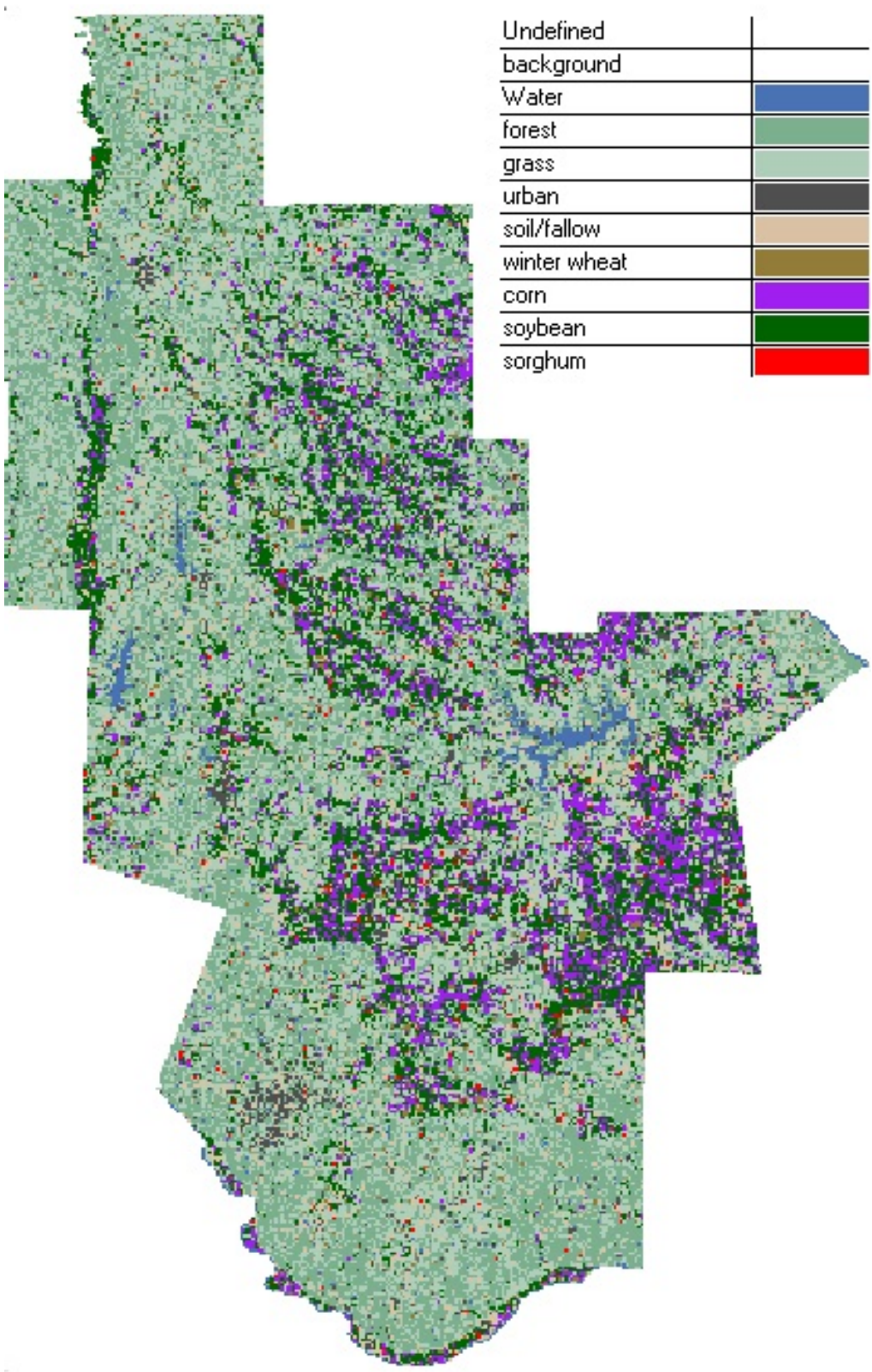

Figure 4.8 Salt River Basin watershed crop map (2005).

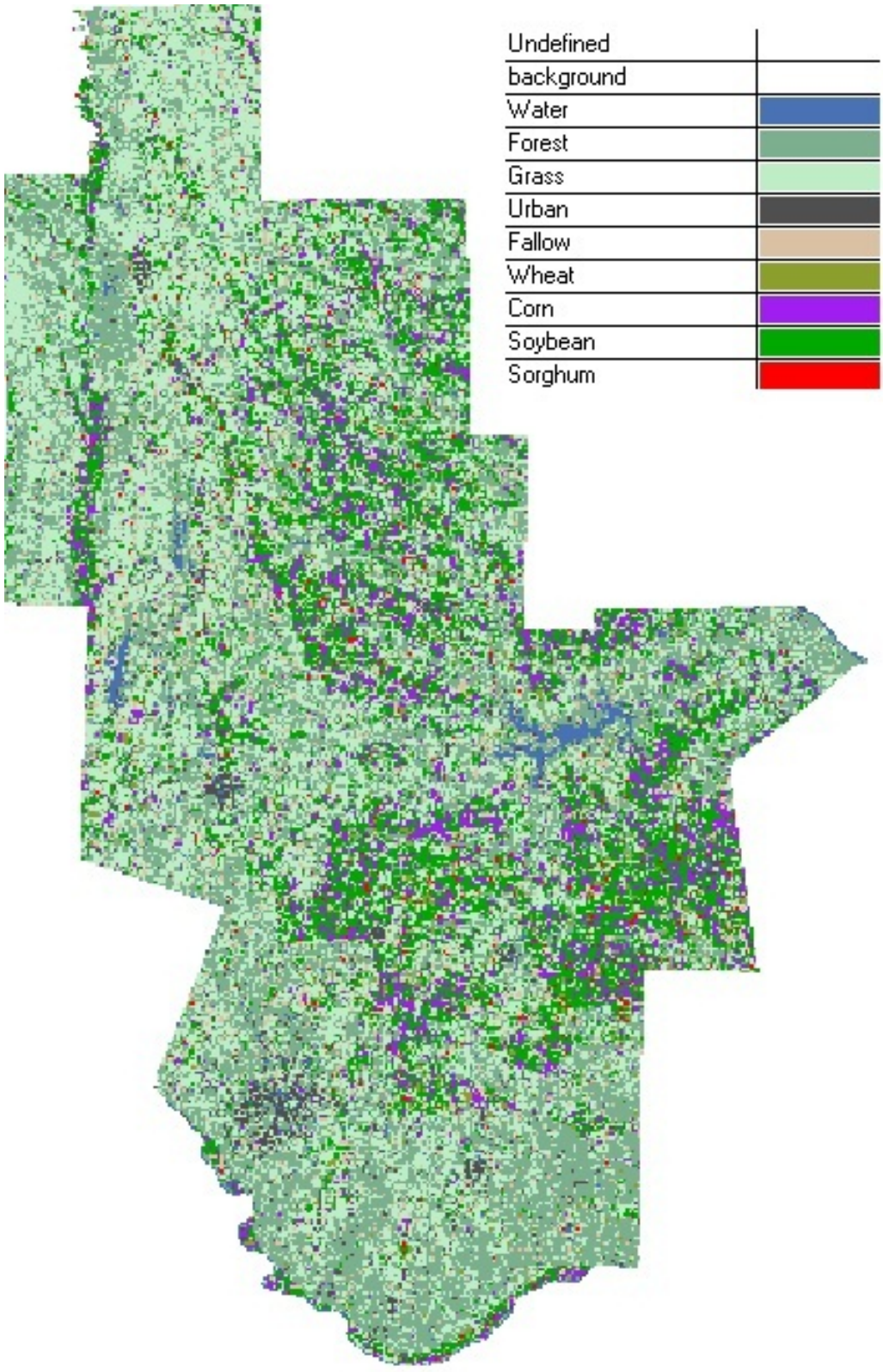

Figure 4.9 Salt River Basin watershed crop map (2006).

Chapter 5

SUMMARY AND CONCLUSION

Three objectives of this study were accomplished. Decision tree and unsupervised classification were used in this study. The crop phenological behaviors in the Salt River watershed were analyzed with the weather influence from Farm Fact report and NDVI profile curves devived from MODIS NDVI data. The procedure developed in this study enables the use of Landsat images to discriminate crop types in Salt River Basin.

The products from two different years which had two different kinds of data source (in growth season and late growth season) expressed the importance of which period of time would be the optimal period to classify each crop type. Data in May and June was useful to classify winter wheat and summer crops. Additional data from July were useful to separate grass/hay from winter wheat. Data from August and early September were the best choice to classify summer crops. But if there was a lack of data in August, the data in July can be used but requires more careful analysis. Weather conditions are important. Dry conditions may reduce NDVI values as well as decrease the time needed to reach the senescence stage and aid farmers in harvesting. Rainfall may make crops grow faster and mature earlier than normal, but may postpone the harvesting operation.

The overall accuracy of the 2005 crop map is good enough for further use. The 2005 crop map could not be verified without field data collected from the USDA ARS. The high accuracy confirmed the decision tree hypotheses the author used in this study, especially in the procedure of classifying grain sorghum from other crops. Correctly discriminating between grain sorghum and soybean is highly desirable in studies about the influence of

fertilizer and pesticides in the Salt River Basin, due to the fact that different chemicals are used with these two crops.

This study concentrated on the classification between crop types, with less analysis on classification between urban, soil and fallow, all which have low NDVI value and high brightness. A better land cover map would be required for further analysis to classify these groups. Also, there were some mixed pixels between grass, not used for hay and forest, which both have high NDVI during summer period.

5.1 Future work

The method of analyzing both the unsupervised class from Landsat images and NDVI values derived from Landsat requires more analysis than other methods, because more variables are used. This method showed a good result with limited Landsat images during the growth season. However, the threshold values applied in the decision tree were chosen from 30 samples of each crop type in the area. Future research is suggested to include statistical analysis of more ground-truth samples to build the NDVI profile representing the crop phenological behavior in the area. MODIS NDVI is useful to analyze crop growth trends. However, the spatial resolution is a weakness for applying MODIS for watershed-scale projects. A recommendation for future research is to analyze the relationship between Landsat NDVI and MODIS NDVI to build crop NDVI profiles with Landsat resolution and better threshold selection.

This method could be applied in previous years when in-season good cloud-free Landsat data were not available. However, weather surveys should be obtained to determine threshold values over time for variables in the decision tree model. The coarse resolution

imagery available from MODIS and AVHRR sensors may be very effective for large-area land cover mapping; however, it needs to be combined with other medium resolution imagery available such as Landsat or SPOT to provide a significant amount of detail and information as is needed in watershed-scale studies.

APPENDIX A

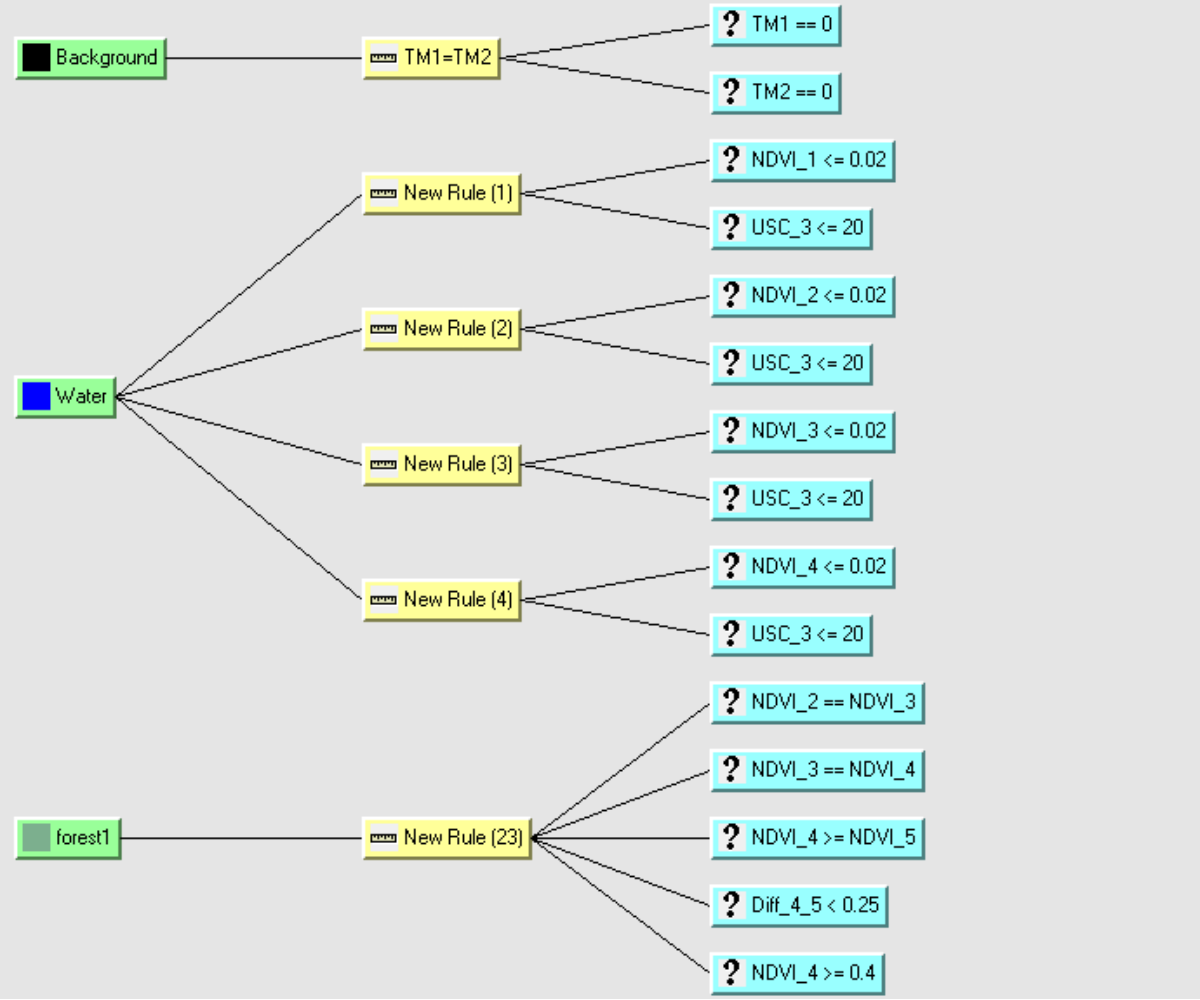

Figure A.1 Decision tree for 2005 crop map.

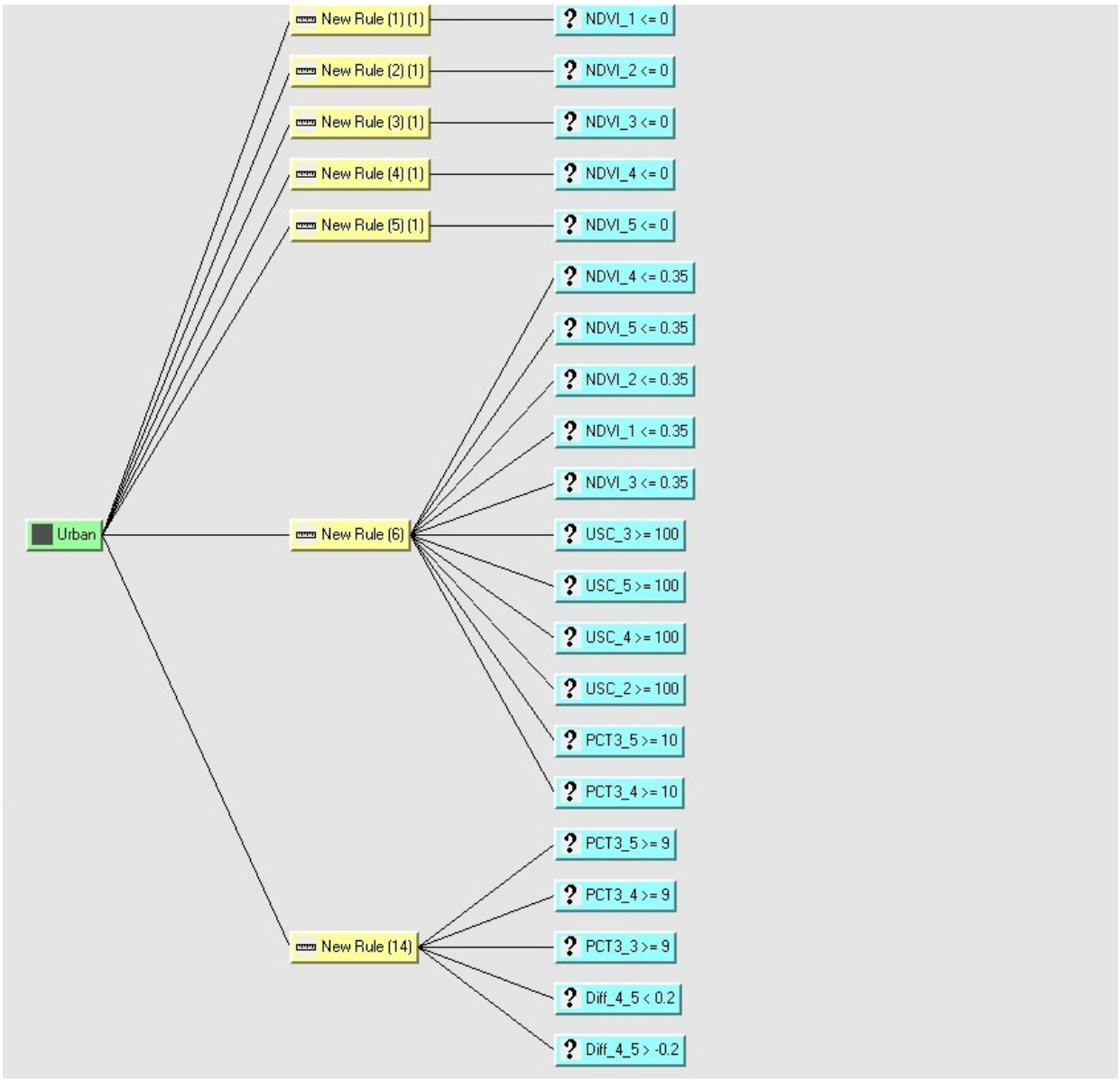

Figure A.1 Decision tree for 2005 crop map (cont).

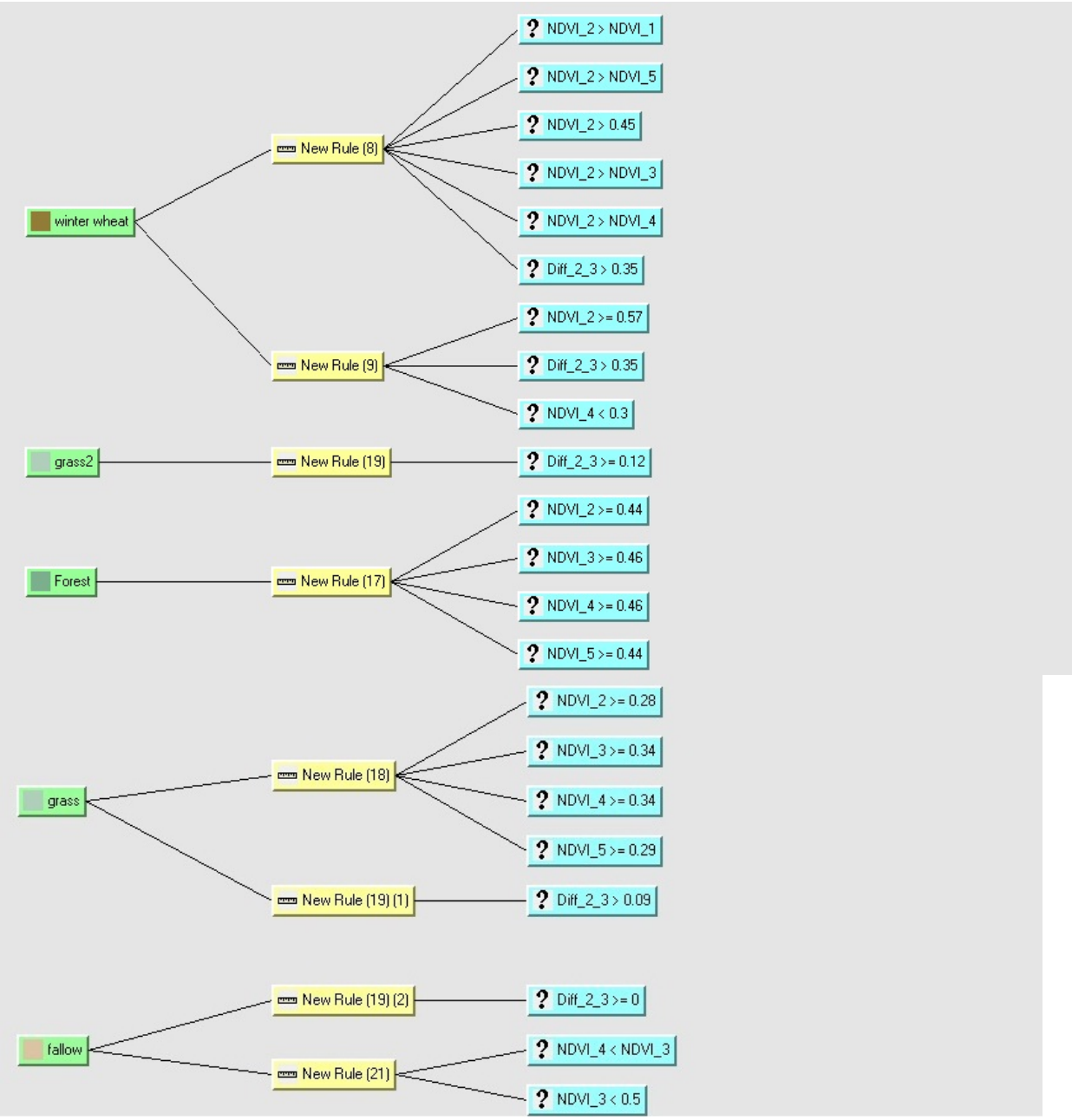

Figure A.1 Decision tree for 2005 crop map (cont).

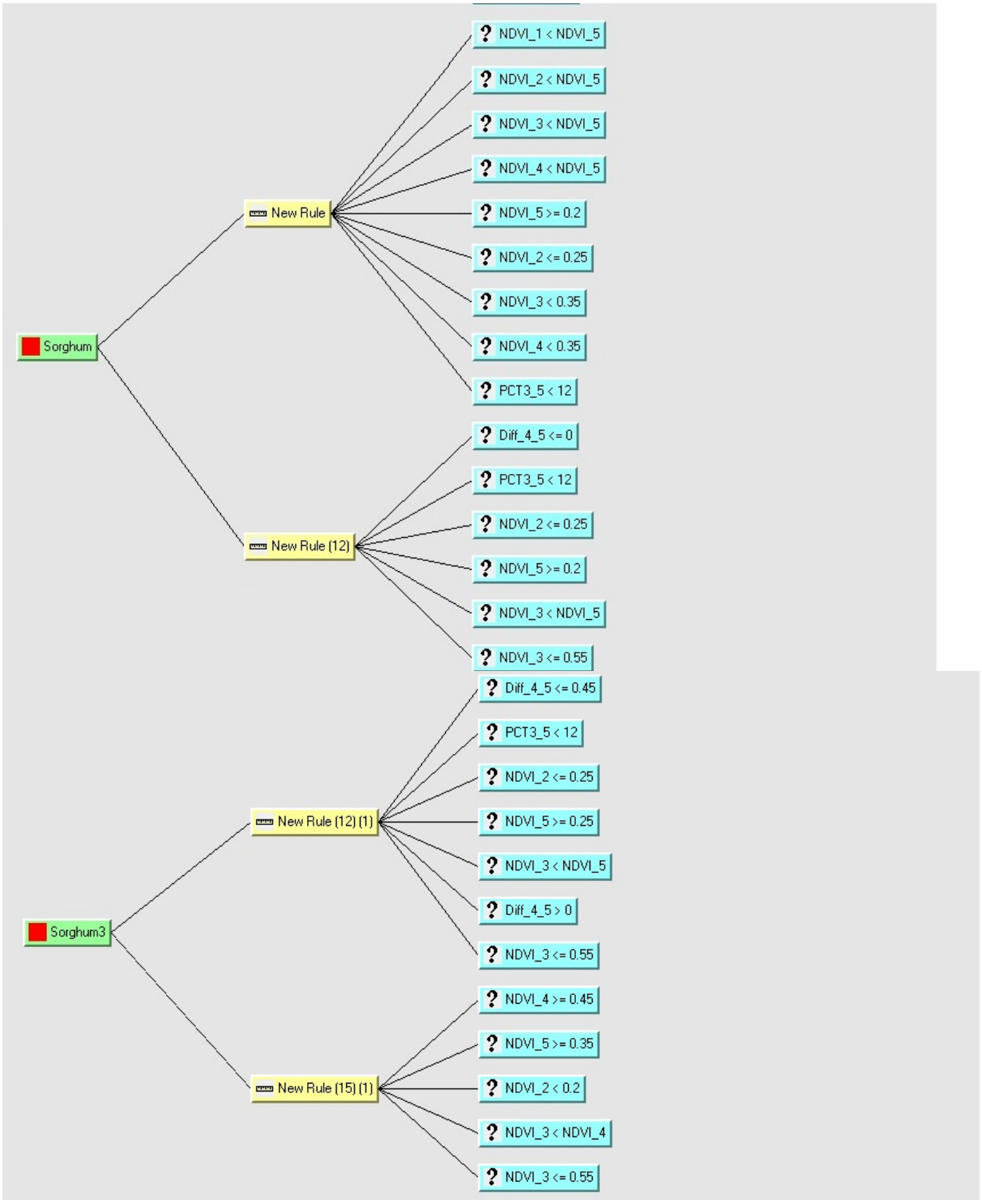

Figure A.1 Decision tree for 2005 crop map (cont).

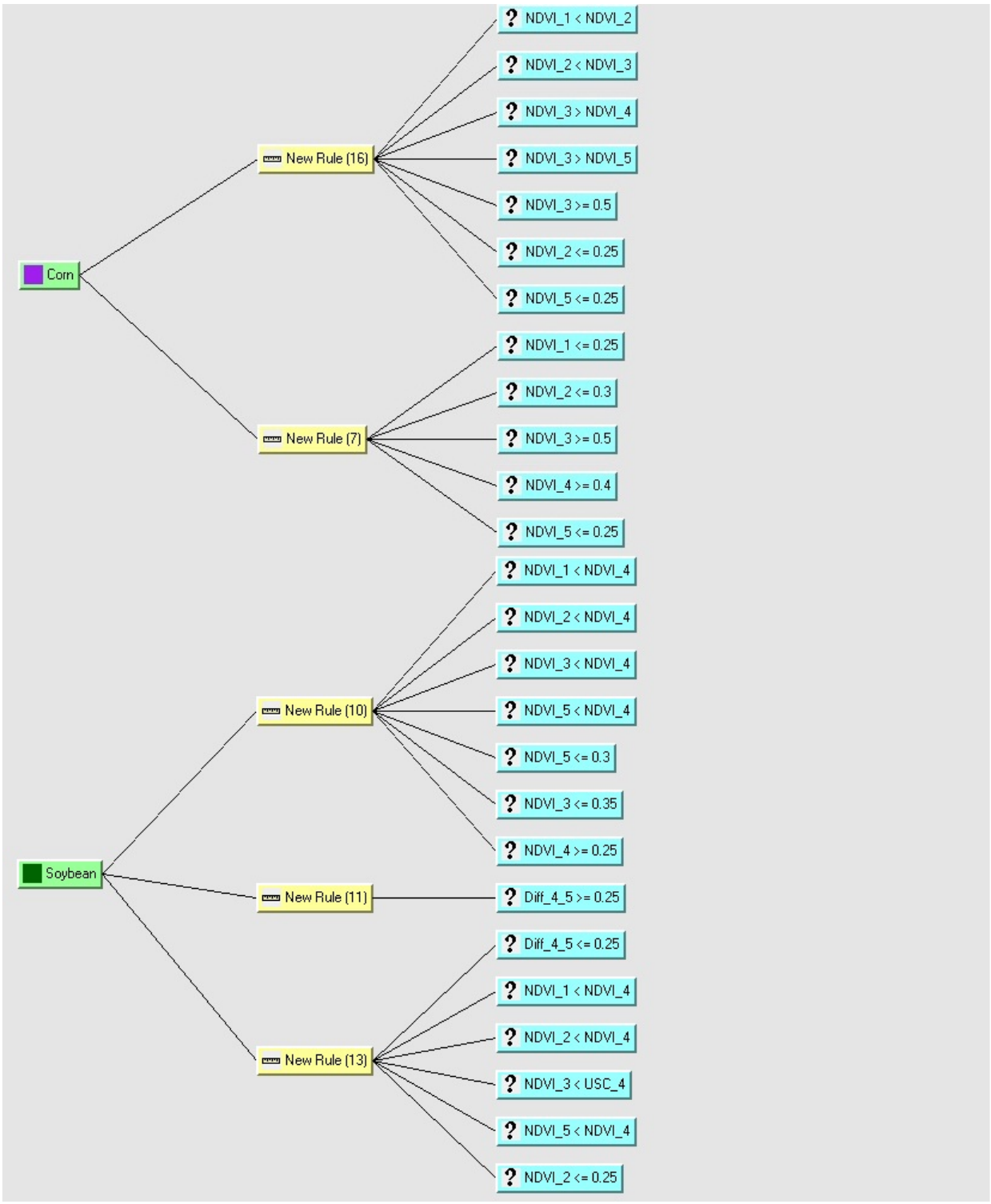

Figure A.1 Decision tree for 2005 crop map (cont).

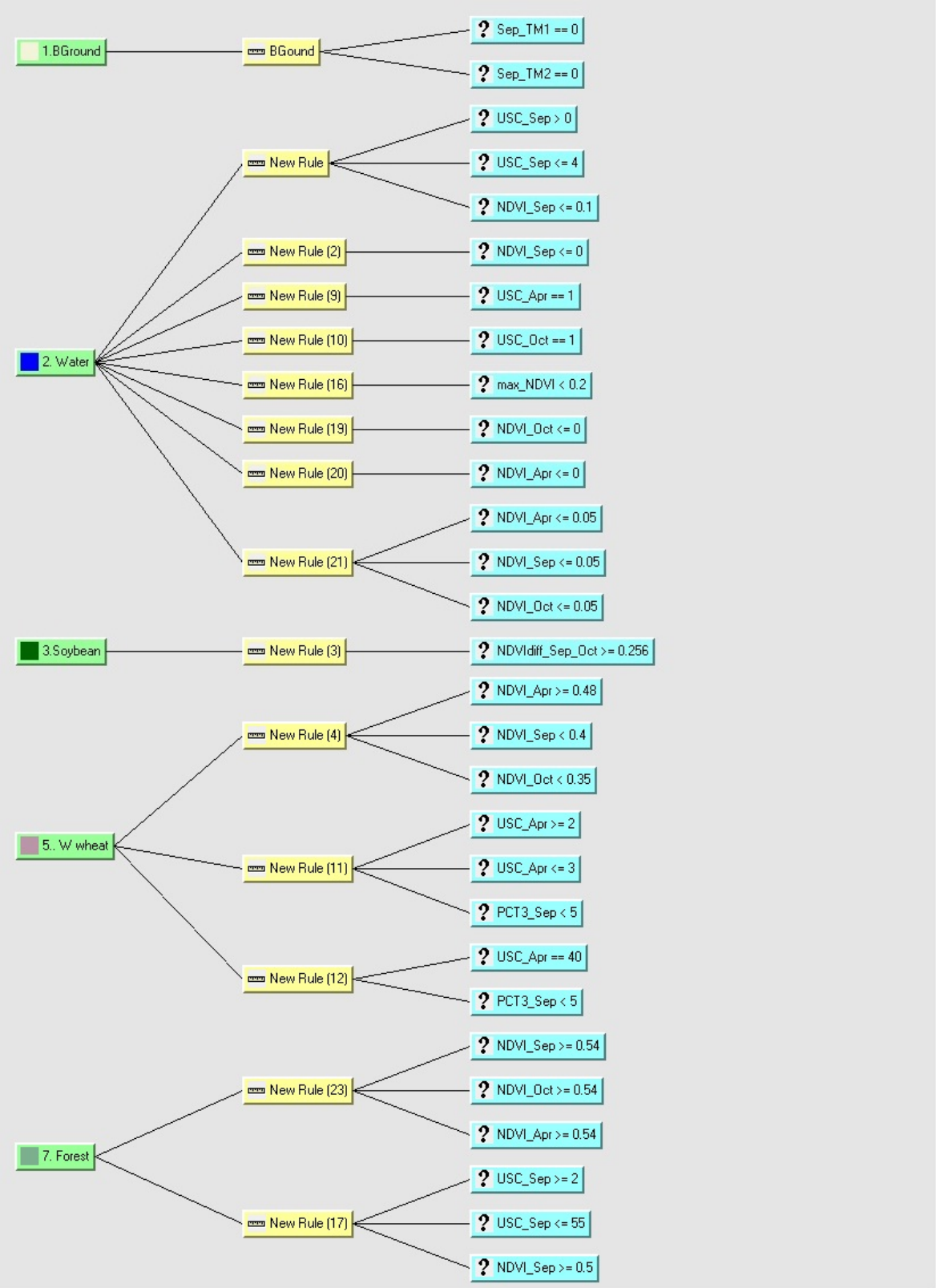

Figure A.2 Decision tree for 2006 crop map.

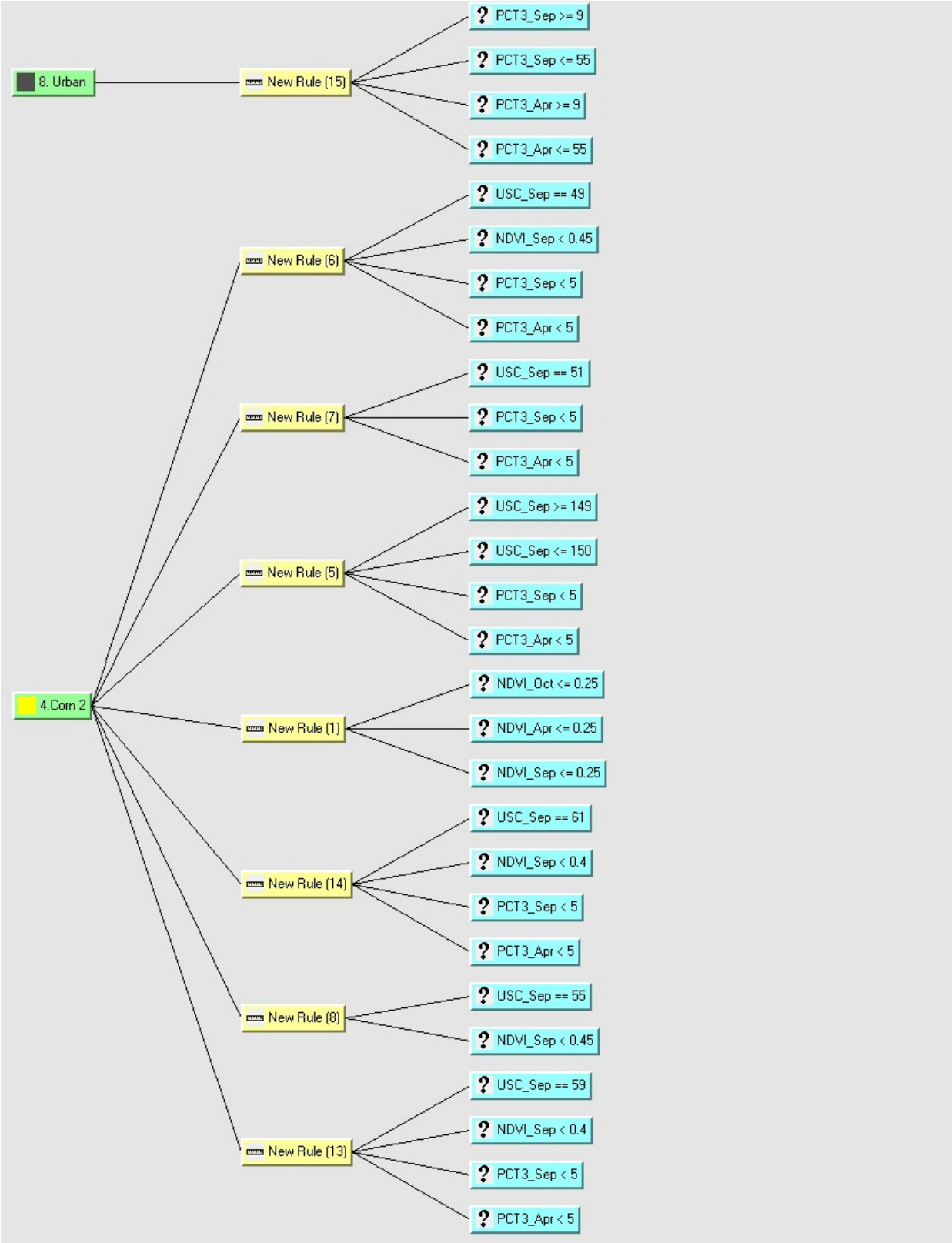

Figure A.2 Decision tree for 2006 crop map (cont).

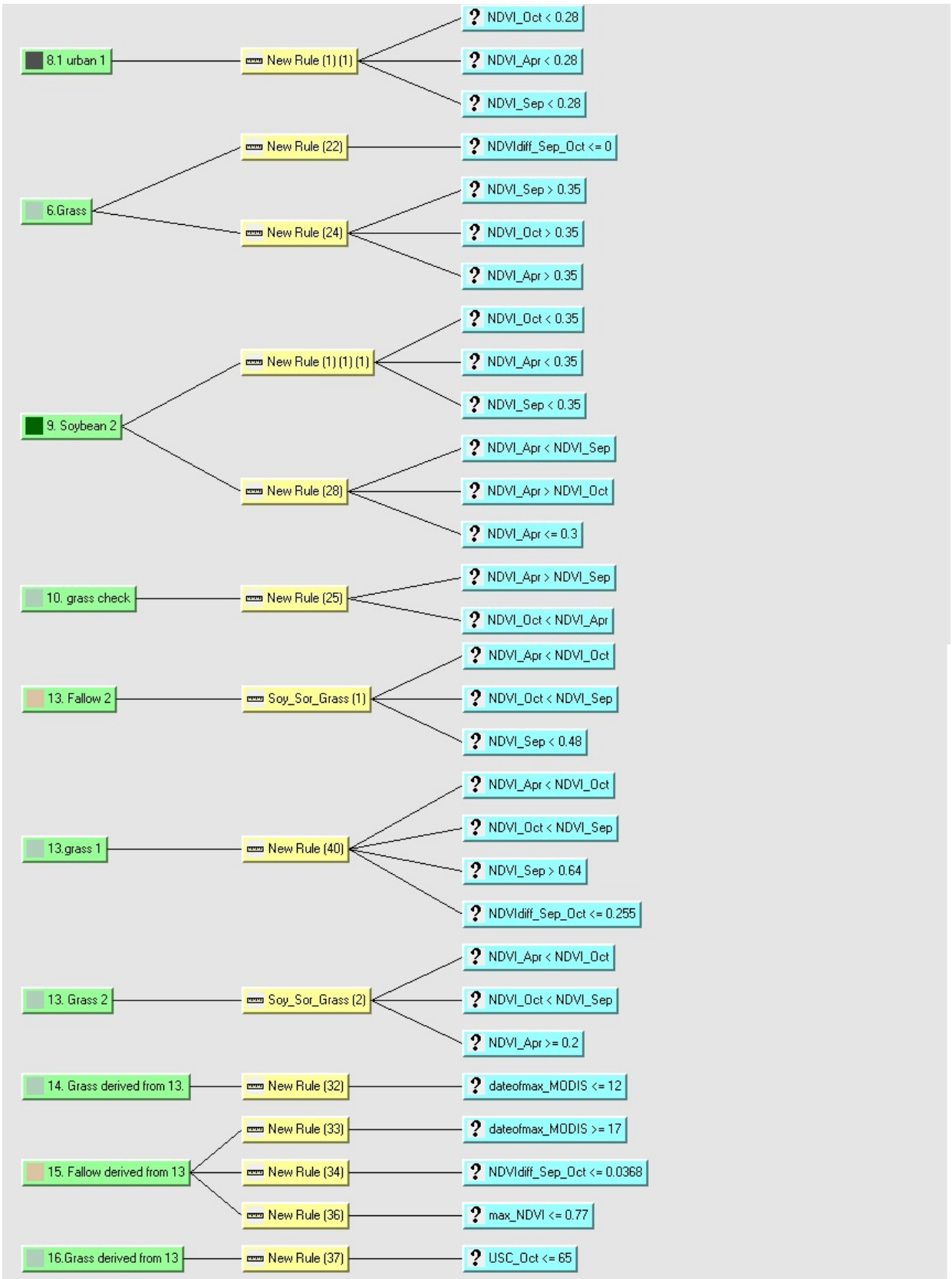

Figure A.2 Decision tree for 2006 crop map (cont).

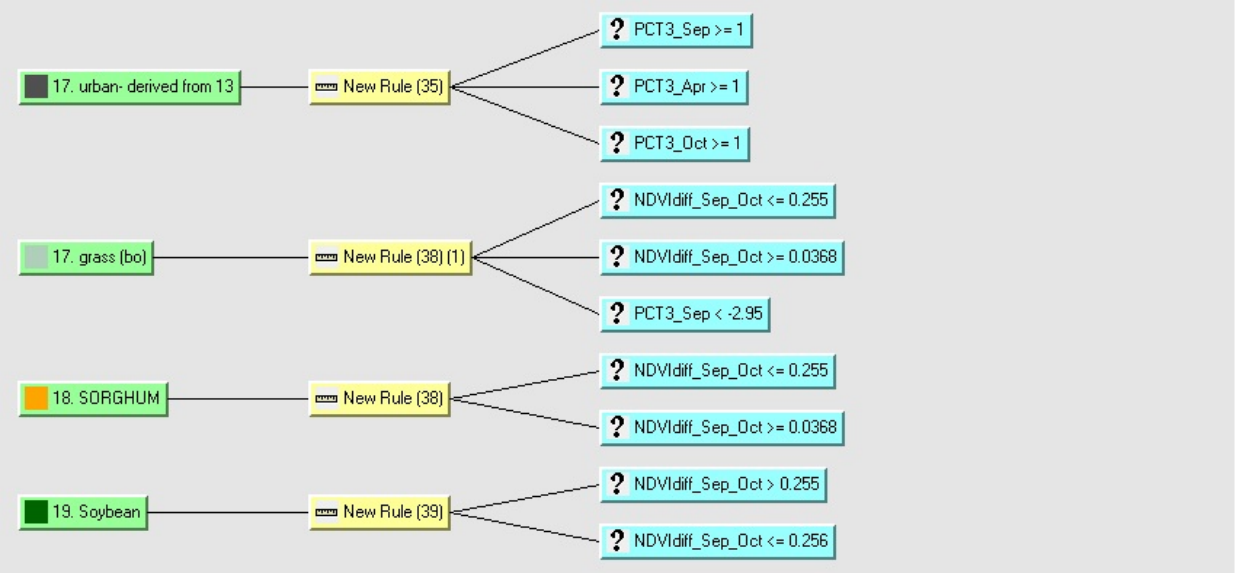

Figure A.2 Decision tree for 2006 crop map (cont).

APPENDIX B

Figure B.1 Goodwater creek Sub-basin 2005.

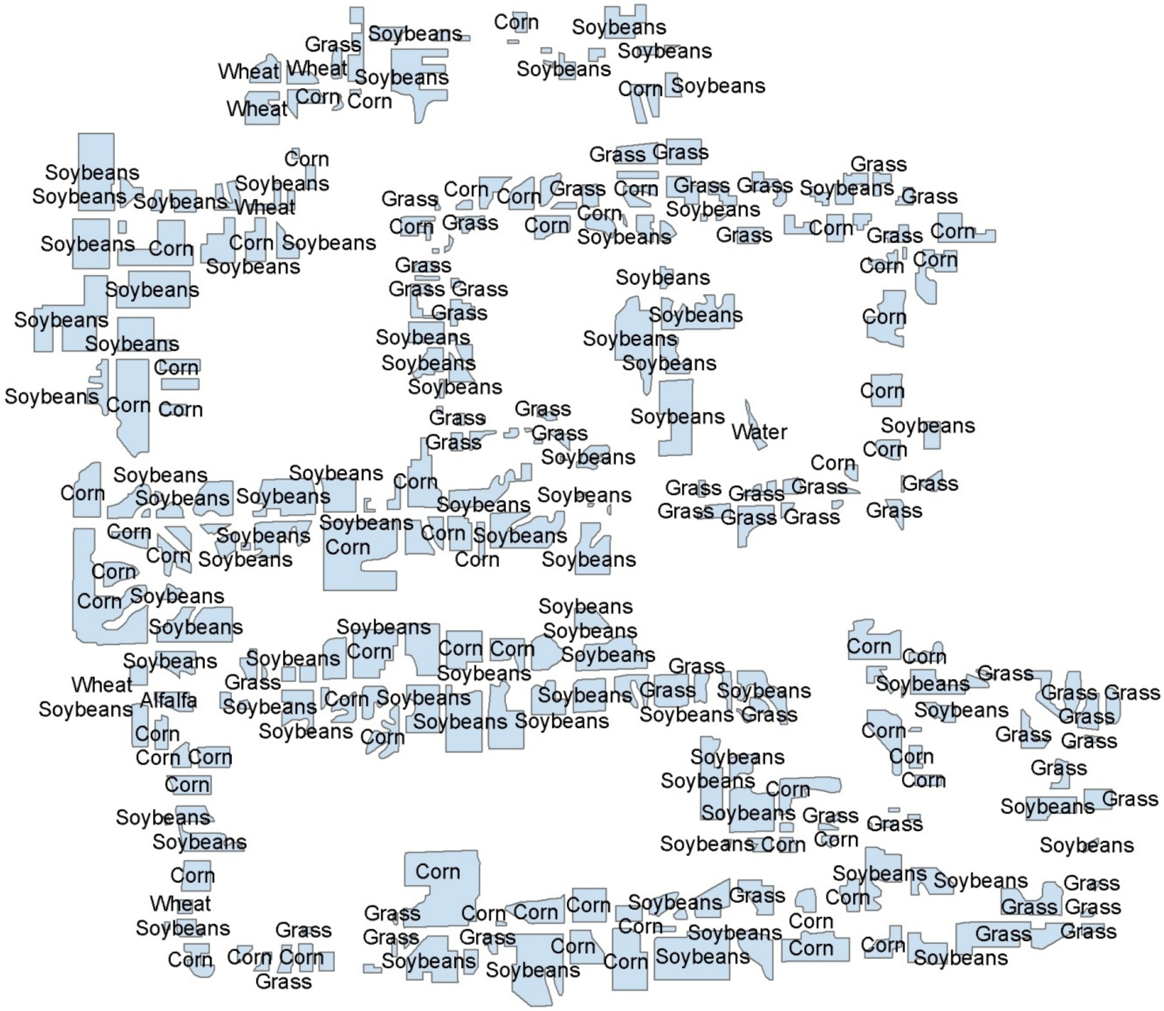

Figure B.2 Greenley reference area 2005.

Figure B.3 Goodwater creek Sub-basin 2006.

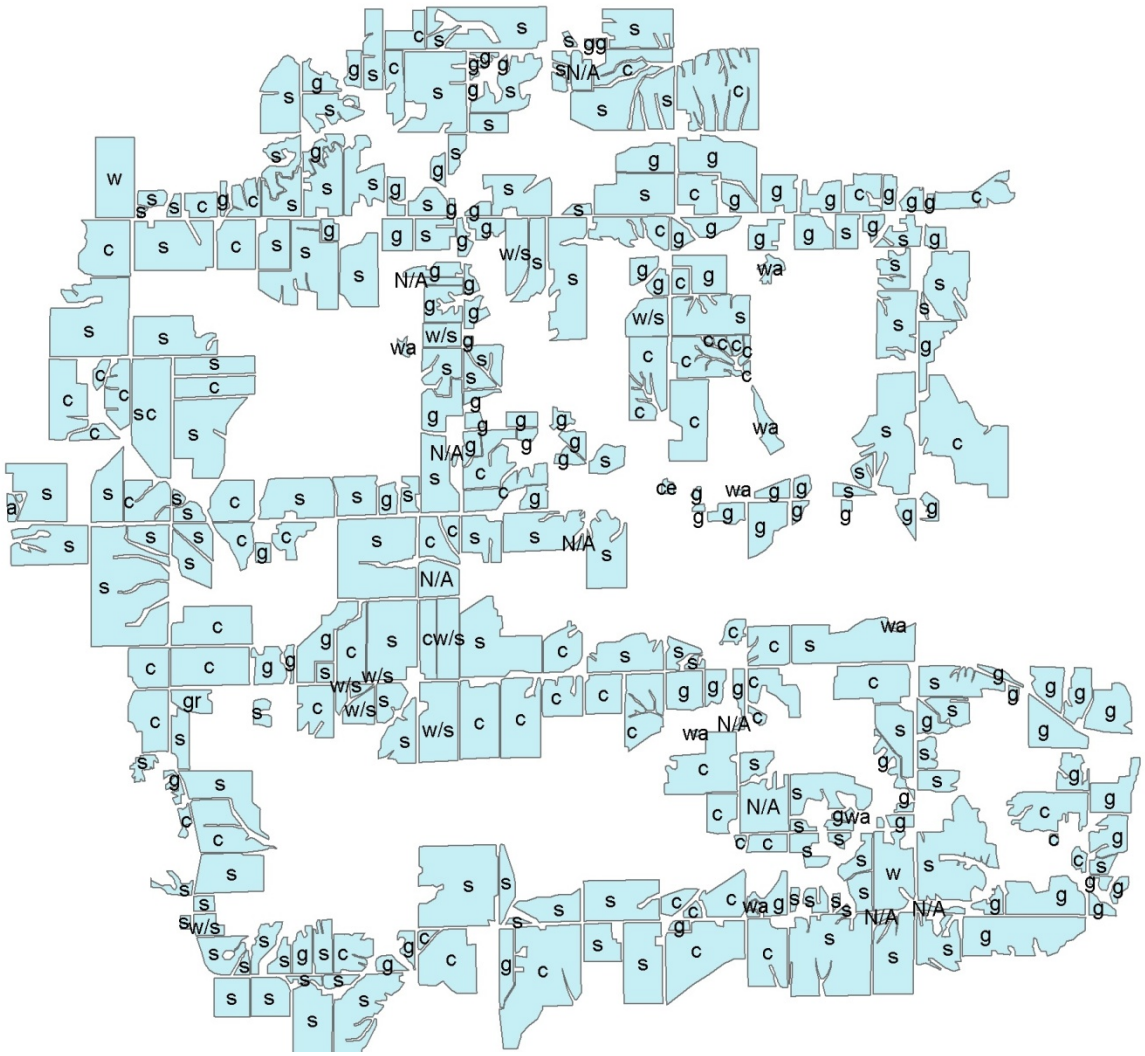

Figure B.4 Greenley reference area 2006.

APPENDIX C

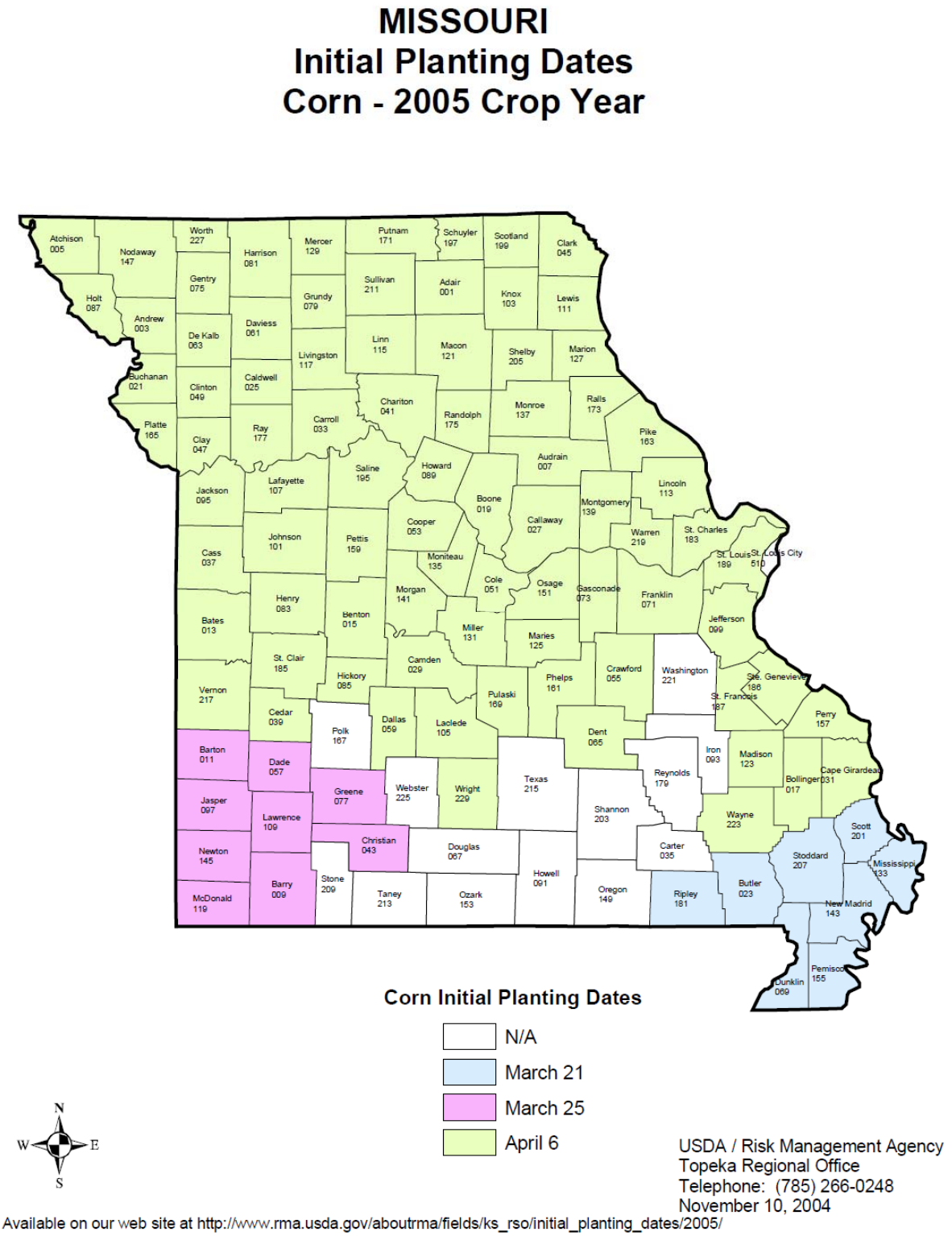

Figure C.1 Missouri Initial planting dates – corn – 2005 crop year

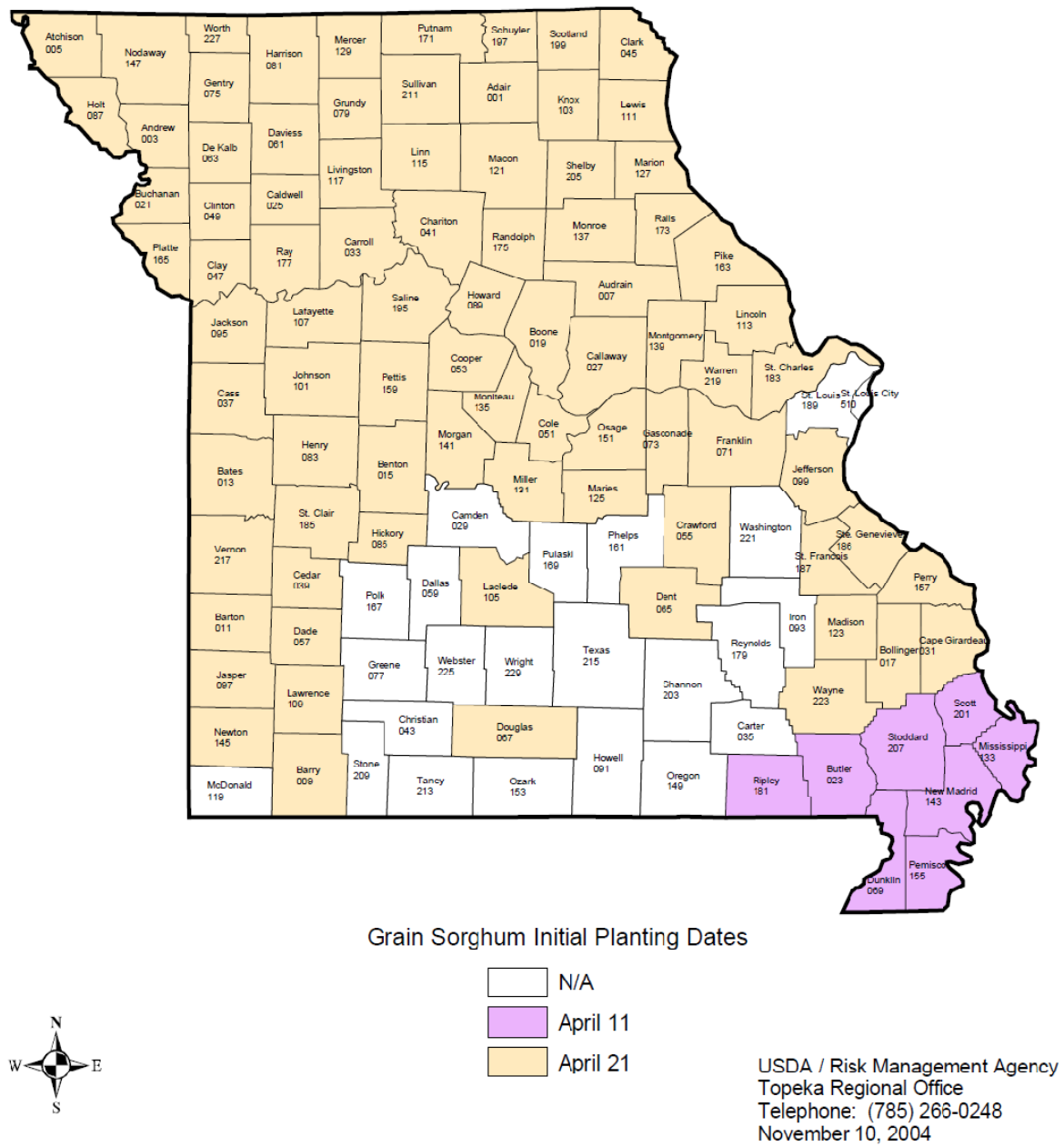

Figure C.2 Missouri Initial planting dates – grain sorghum – 2005 crop year.

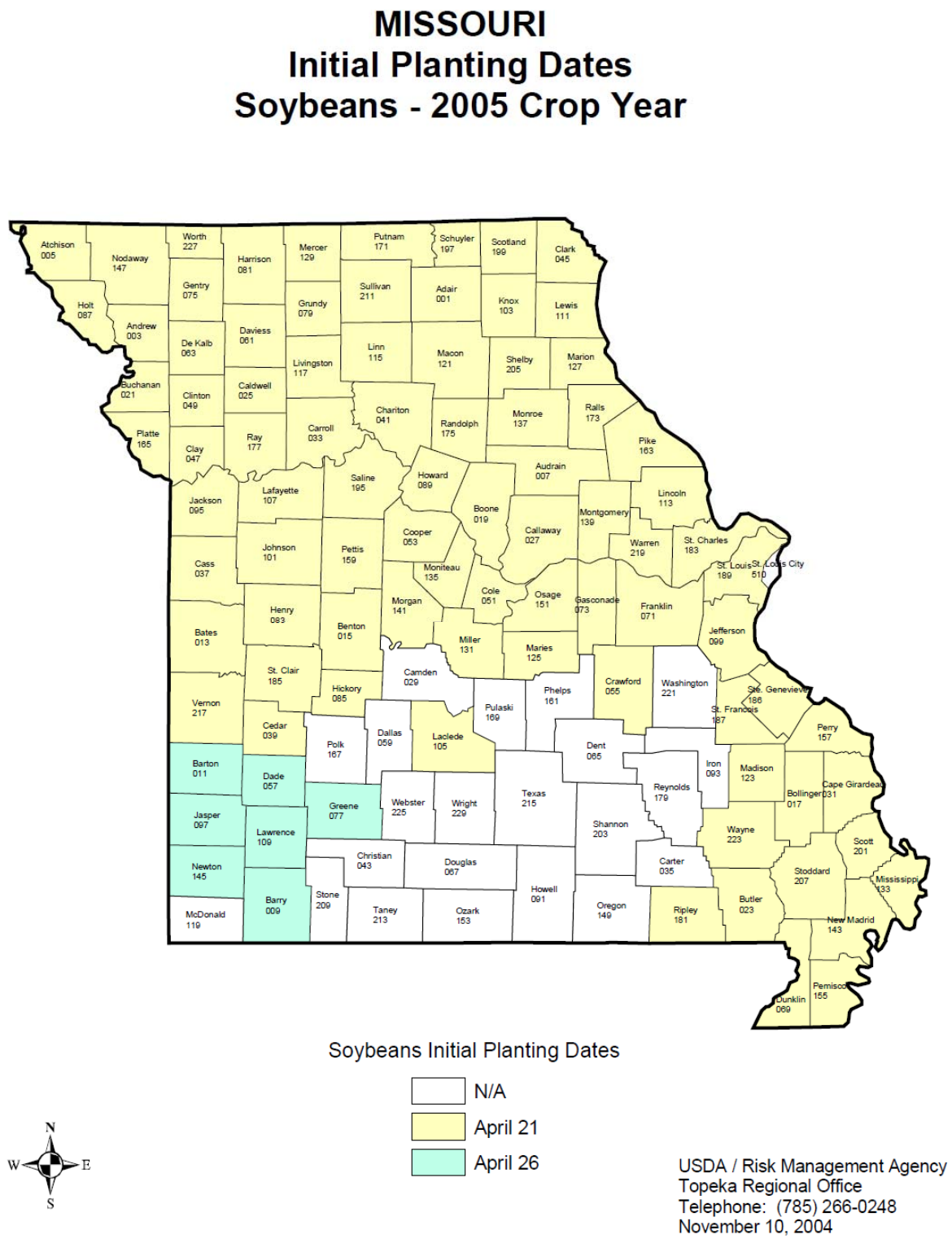

Figure C.3 Missouri Initial planting dates – soybean – 2005 crop year.

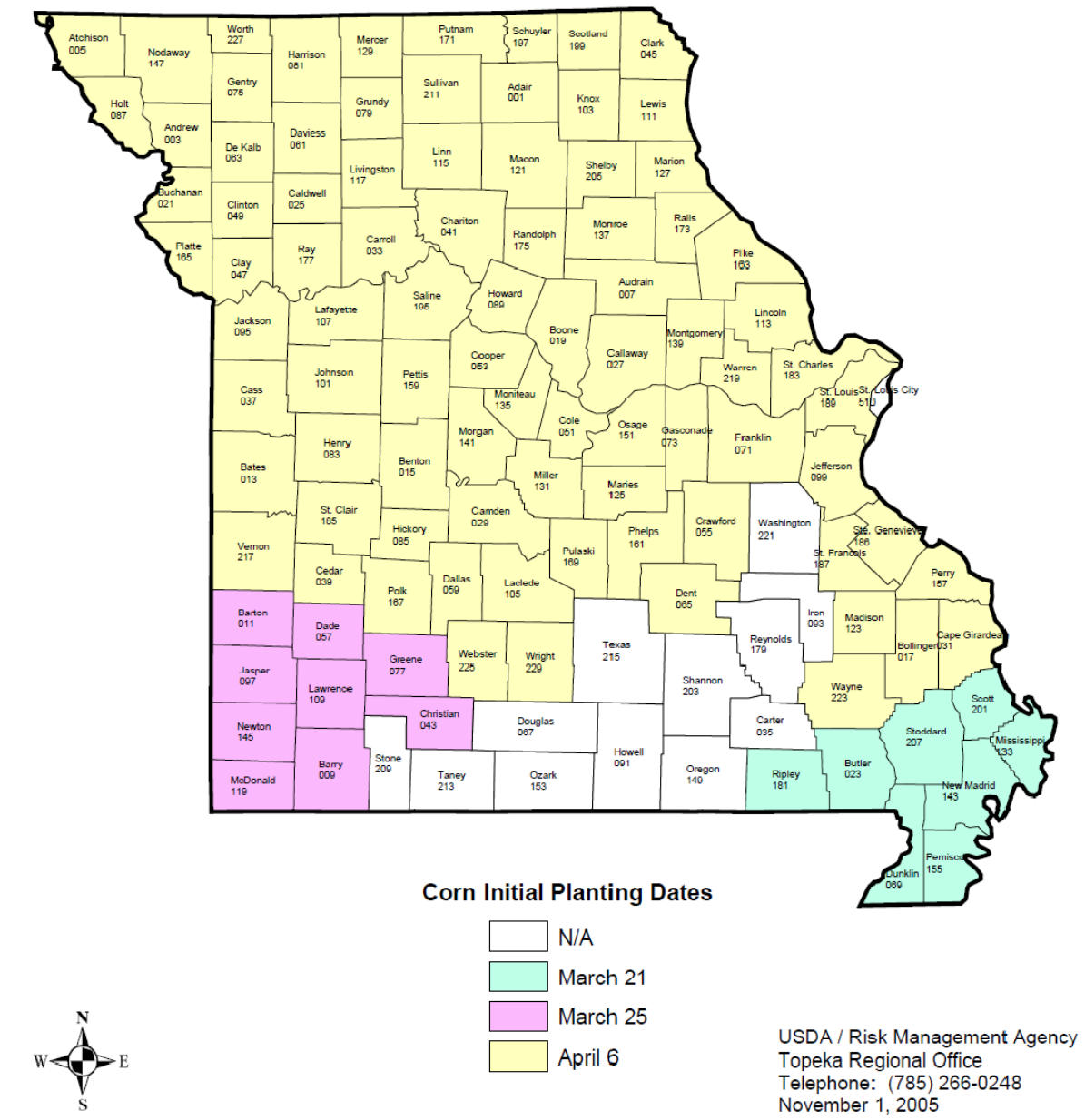

Figure C.4 Missouri Initial planting dates – corn – 2006 crop year.

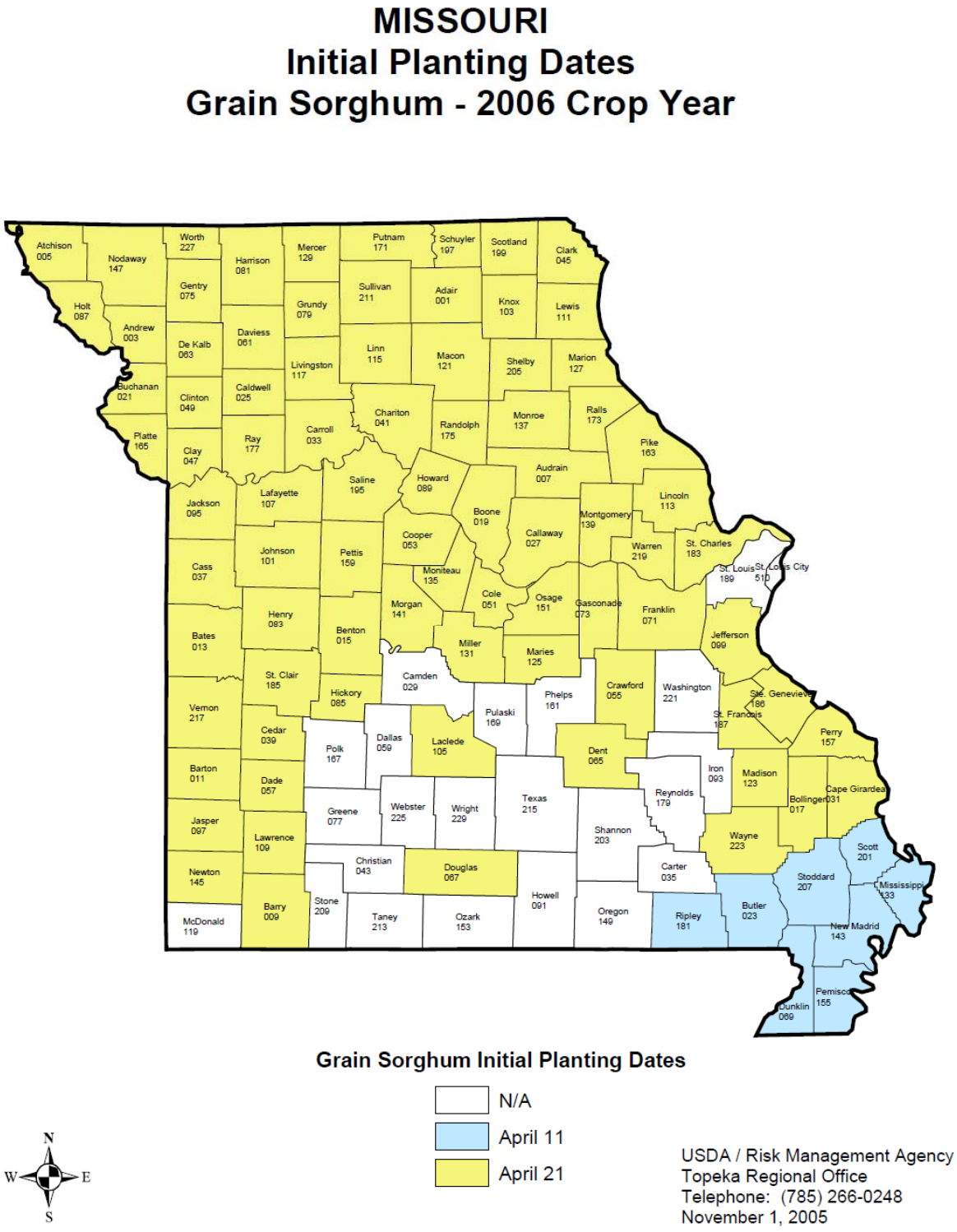

Figure C.5 Missouri Initial planting dates – grain sorghum – 2006 crop year.

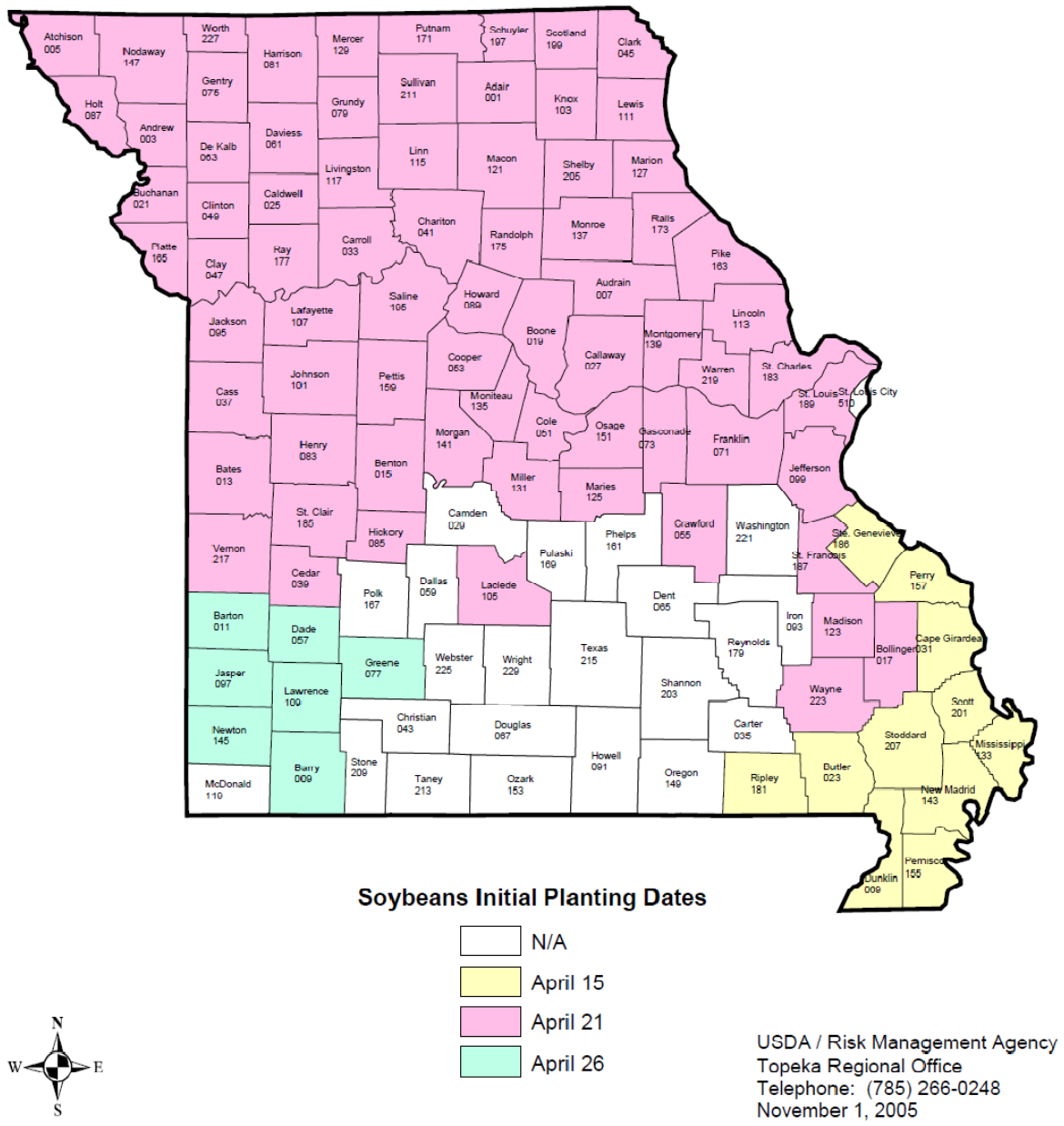

Figure C.6 Missouri Initial planting dates – soybean – 2006 crop year.

REFERENCES

Agrawal. S., P.K. Joshi, Y. Shukla and P.S. Roy. 2003. SPOT VEGETATION multitemporal data for classifying vegetation in south central Asia. Current Science. 84(11): 1440-1448.

Aplin, P. and P.M. Atkinson. 2001. Sub-pixel land cover mapping for per-field classification. International Journal of Remote Sensing. 22(14): 2853-2858.

Bauer, M.E. 1985. Spectral inputs to Crop Identification and Condition Assessment. Proceedings of the IEEE. 73(6): 1071-1085.

Brook, R. K., and N.C. Kenkel. 2002. A multivate approach to vegetation mapping of Manitoba's Hudson Bay Lowlands. International Journal of Remote Sensing. 23(21): 4761-4776.

Choubey,V.K. and Subramanian. 1992. Estimation of suspended solids using India Remote Sensing Satellite- 1A data: a case study from Central India. International Journal of Remote Sensing. 13(8): 1473-1486.

Chubey, M.S., S.E. Franklin and M.A. Wulder. 2006. Object-based Analysis of Ikonos-2 Imagery for Extraction of Forest Inventory Parameters. Photogrammetric Engineering & Remote Sensing. 72(4): 383-394.

Cihlar, J. 2000. Land cover mapping of large area from satellite: status and research priorities. International Journal of Remote Sensing. 21(6-7): 1093-1114.

Cohen, Y. and M. Shoshany. 2002. A national knowledge-based crop recognition in Mediterranean environment. International Journal of Applied Earth Observation and Geoinformation. 4: 75-87.

Collingwood, A. 2008. Satellite Image Classification and Spatial Analysis of Agricultural Areas for Land Cover Mapping of Grizzly Bear Habitat. MS Thesis. University of Saskatchewan Saskatoon, Canada. 136 pp.

Congalton, G. R. 1991. A review of Assessing the accuracy of Classifications of Remotely Sensed data" Remote Sensing of Environment. 37: 35-46.

Craig, M. E. 2001. The NASS cropland data layer program. Presented at the third International Conference on Geospatial Information in Agriculture and Forestry. Denver, CO.

Crist, E.P. and R.C. Ciccone. 1984. A physically-based transformation of thematic mapper data-the TM tasseled cap. IEEE Transactions on Geoscience and Remote Sensing. 22: 256-263.

DeFries, R.S. and A.S. Belward. 2000. Global and regional land cover characterization from satellite data: An introduction to the special issue. International Journal of remote sensing. 21(6-7): 1083-1092.

De Wit, A.J.W. and J.G.P.W. Clevers. 2004. Efficiency and accuracy for per-field classification for operational crop mapping. International Journal of Remote Sensing. 25(20): 4091-4112.

Doraiswamy, C. P., B. Akhmedov, L. Beard, A. Stern and R. Mueller, 2006a. Operational prediction of crop yields using MODIS data and products. ISPRS Archives XXXVI-8/W48 Workshop proceedings: Remote sensing support to crop yield forecast and area estimate.

Doraiswamy, C. P., B. Akhmedov, L. Beard, A. J. Stern 2006b. Improved Techniques for Crop Classification using MODIS Imager, International Geoscience and Remote Sensing Symposium, pp. 2084-2087.

Finney, V.L., 1986. Seasonal sediment yield to Mark Twain Lake, Missouri. Bulletin of the Association of Engineering Geologist. 23(3): 333-338.

Foody, G.M., 2002. Status of land cover classification accuracy assessment. Remote Sensing of Environment. 80: 185-201.

Franklin, S.E. 2001. *Remote sensing for sustainable forest management*. Boca Raton FL: CRC/Lewis Press.

Franklin, S.E. and M.A. Wuller. 2002. Remote sensing methods in medium spatial resolution satellite data land cover classification of large areas" Progress in Physical Geography, vol. 26, no. 2, 2002, pp. 173-205.

Fried, M.A., C.E. Brodley and A.H. Strahler, 1999. Maximizing land cover classification accuracies produced by decision trees at continental to global scales. IEEE Transactions on Geoscience and Remote Sensing. 37: 969-977.

Ghidey, F., E.J. Sadler, R.N. Lerch, and C. Baffaut. 2005. Simulating hydrology and water quality of a clayoan soil watershed. ASABE Paper No. 052084. St Joseph, MI: American Society of Agricultural Engineers.

Ghidey, F., E.J. Sadler, R.N. Lerch, and C. Baffaut. 2007. Scaling up the SWAT model from Goodwater Creek Experimental Watershed to the Long Branch Watershed. ASABE Paper No. 072043. St Joseph, MI: American Society of Agricultural Engineers.

Harry, C. M. and W.J. Wiebold. 1949. Wheat-Soybean Double-crop Management in Missouri. MU extension, University of Missouri-Columbia.

Havlin, J., A. Schlegel, K.C. Dhuyvetter, J.P. Shroyer, H. Kok, and D. Peterson. 1995. Great plains dryland conservation technologiesPublication. S-81: pp. 711. Manhattan, KS: Kansas State University.

Homer, C., C. Huang, L. Yang, B. Wylie and M. Coan. 2004. Development of a 2001 national land-cover database for the United States. Photogrammetric Engineering and Remote Sensing, 70(7): 829-840.

Huete, A.R., 1988. A soil-adjusted vegetation index (SAVI). Remote Sensing Environment. 25: 295-309.

Huete, A.R. and C. Justive. 1999. MODIS vegetation index (MOD 13): Algorithm theoretical basis document (pp. 43-46). Tucson, Arizona: University of Arizona.

Jackson, J. Thomas, Daoyi Chen, Michael Cosh, Fuqin Li, Martha Anderson, Charles Walthall, Paul Doraiswamy, E. Ray Hunt. 2004. Vegetation water content mapping using Landsat data derived normalized difference water index for corn and soybeans. Remote Sensing of Environment, 92: 475-782.

Jang, G. S., K. A. Sudduth, E. J. Sadler and R. N.Lerch. 2009. Watershed-scale type classification using seasonal Trends in remote sensing-derived vegetation indices. American Society of Agricultural and Biological Engineers. 52(5): 1535-1544.

Jensen, J.R., Remote Sensing of the Environment: An Earth Resource Perspective. Upper Saddle River, Prentice Hall, 2000.

Jianqiang, R., Z. Chen, Q. Zhou and H. Tang "Regional yield estimation for winter wheat with MODIS –NDVI data in Shandong, China" International Journal of Applied Earth Observation and Geoinformation vol. 10, 2008, pp. 403-413.

Jiyul, C., M. C. Hansen, K. Pittman, M. Corroll, and C. DiMiceli 2007. Corn and Soybean Mapping in the United State Using MODIS Time-Series Data Sets. Agronomy Journal.99: 1654-1664.

Joshi, P.K.K., P.S. Roy, S. Singh, S. Agrawal, and D. Yadav. 2006. Vegetation cover mapping in India using multi-temporal IRS Wide Field Sensor (WiFS) data. Remote Sensing of Environment. 103: 190-202.

Kauth, R.J. and G.S. Thomas. 1976. The tasseled cap – a graphic description of the spectral-temporal development of agricultural crops as seen by Landsat. Pages 4B-41 – 4B-51 in Swain PH, Morrison DB, eds Processing of Remotely Sensed Data, Purdue University Laboratory for Applications of Remote Sensing, West Lafayette, IN, 6 June – 2 July 1976. New York: Institute of Electrical and Electonics Engneers.

Kaufman J. Y., D. Tanre 1992. Atmospherically Resistant Vegetation Index (ARVI) for EOS-MODIS. IEEE Transactions on Geoscience and Remote Sensing. 30(2): 261-270.

Kawata, Y., A. Ohtani, T. Kusaka and S. Ueno. 1990. Classification accuracy for the MOS-1 MESSR data before and after the atmospheric correction. IEEE Transactions on Geoscience and Remote Sensing. 28: 755-760.

Lillesand, M. T., R.W. Kiefer, J.W. Chipman, 2004. Remote Sensing and Image Interpolation, 5th Edition, John Wiley & Sons.

Lerch, E.N., E.J. Sadler, N.R. Kitchen, K.A. Sudduth, E.J. Kremer, D.B. Myers, C. Baffaut, S.H. Anderson and C.H. Lin. 2008. Overview of the Mark Twain Lake/Salt River Basin Conservation Effects Assessment Project. Journal of Soul and Water Conservation. 63(6): 345-359.

Lodhi, M.A., D.C. Rundquist, L.Han and M.S. Kuzila. 1997. The potential for remote sensing of loess soils suspended in surface waters. Journal of the American Water Resources Association. 33(1): 111-117.

Lyon, J.G., K.W. Bedford, C.J. Yen, D.H. Lee and D. J. Mark. 1988. Determinations of suspended sediment concent5rations for multiple day Landsat and AVHRR data. Remote Sensing of Environment. 25: 107-115.

McIver, D.K., and M.A. Friedl. 2002. Using prior probabilities in decision tree classification of remote sensed data. Remote Sensing of Environment. 81: 253-261.

Missouri Initial Planting Dates 2005, USDA, Risk Management Agency: www.rma.usda.gov/aboutrma/fields/ks_rso/initial_planting_datas/2005/

Missouri Initial Planting Dates 2006, USDA, Risk Management Agency: http://www.rma.usda.gov/aboutrma/fields/ks_rso/initial_planting_dates/2006/

Mosiman, B. 2003. Exploring Multi-Temporal and Transformation Methods for Improved Cropland Classification Using Landsat Thematic Mapper Imagery. Master's Thesis, Department of Geography, University of Kansas, Lawrence, KS.

Mueller, R., C. Boryan, R. Seffrin. 2009. Data Partnership Synergy: The cropland Data Layer. US Department of Agriculture, National Agricultural Statistics Service. Fairfax, VA.

Murthy, C.S, P.V. Raju and K.V.S. Badrinath. 2003. Classification of wheat crop with multi-temporal images: performance of maximum likelihood and artificial neural networks. International Journal of Remote Sensing. 24(23): 4871-4890.

Reese, H.M, T.M. Lillesand, D.E. Nagel, J.S. Stewart, R.A. Goldmann, T.E. Simmons, J.W. Chipman and P.A. Tessar. 2002. Statewide land cover derived from multi-seasonal Landsat TM data: A retrospective of the WISLAND project. Remote Sensing of Environment. 82: 224-237.

Richards, J.A. and X. Jia. 2006. Remote Sensing Digital Image Analysis – An introduction. 4th Edition. Springer. Canberra, Australia.

Rogers, D. H. 1997. Soybean production handbook. Publication, Vol. C-449 (pp. 1519). Kansas State University. Manhattan, KS.

Running, S.W., T.R. Loveland and L.L. Pierce. 1994. A vegetation classification logic based on remote sensing for use in global biogeochemical models. Ambio. 23: 77-81.

SBRC, 1994, Space sensors. Goleta, CA: Santa Barbara Research Center, 33 pp.

Skadeland, T. 1992. Water Quality and Land Cover Types in the Upper Salt River Basin. MS Thesis, University of Missouri-Columbia, 118 pp.

Soil Conservation Service. 1974. Soil survey of Marion and Ralls counties, Missouri. U.S. Government Print. Off. 1979:-207-350/122.

Soil Conservation Service. 1979. Soil survey of Knox, Monroe, and Shelby counties, Missouri. U.S. Government Print. Off. 1979:-207-350/122.

Soil Conservation Service. 1989. Soil survey of Marion and Randolph county, Missouri. U.S. Government Print. Off. 1989: 0-205-522.

Song C., C.E. Woodcock, K.C. Seto, M.P. Lenney, and S.A. Macomber, 2001. Classification and Change Detection Using Landsat TM Data: When and How to correct Atmospheric Effects? Remote Sensing of Environment, 75: 230-244.

Stephen B.A. 2000. Remote Sensing of Suspended Solid and Turbidity in Mark Twain Lake, Missouri. MA Thesis. University of Missouri-Columbia. 112 pp.

Tou, D. L. and R.C. Gozalez. 1974. Pattern Recognition Principles. London, U.K.: Addison-Wesley.

USDA, National Agricultureal Statistic Service, 2005: Quick stats agricultural statistic data base.www.nass.usda.gov/data_and_statistics/

USDA, National Agricultureal Statistic Service, Missouri, Farm Facts publication: http://www.nass.usda.gov/Statistics_by_State/Missouri/Publications/Farm_Facts/

Vanderlip, R., D.H. Rogers and M. Alam. 1998. Grain sorghum production guide. Publication, Vol. C-687. pp. 1518. Kansas State University. Manhattan, KS.

Van Niel, T.G. and T.R. McVicar. 2004. Determining temporal windows for crop discrimination with remote sensing: a case study in south-eastern Australia. Computers and Electronics in Agriculture. 45: 91-108.

Van Niel, T.G., T.R. McVicar and B. Datt. 2005. On the relationship between training sample size and data dimensionality: Monte Carlo analysis of broadband multi-temporal classification. Remote Sensing of Environment. 98: 468-480.

Wang, J., P.M. Rich, K.P. Price, W.D. Kettle, 2005. Relations between NDVI, Grassland Production, and Crop Yield in the Central Great Plains. Geocarto International, 20(3): 5-11.

Wardlow, D.B. and S.L. Egbert 2005. State-level crop mapping in the U.S. Central Great Plains Agroecosystem using MODIS 250-meter NDVI data.

Wardlow, D. B., S.L. Egbert and J.H. Kastens. 2007. Analysis of time-series MODIS 250 m vegetation index data for crop classification in the U.S. Central Great Plains" Remote Sensing of Environment.108: 290-310.

Walter, V. 2004. Object-based classification of remote sensing data for change detection. ISP RS Journal of Photogrammetry & Remote Sensing. 58: 225-238.

Yamamoto, Y., T. Oberthur, R. Lefroy. 2009. Spatial identification by satellite imagery of the crop-fallow rotation cycle in northern Laos. Environ Dev Sustain. 11: 639-654.

Zhang, X., M.A. Friedl, C.B. Schaaf, A.H. Strahler,J.C.F. Hodges, and F. Gao. 2003. Monitoring vegetation phenology using MODIS. Remote Sensing of Environment. 84: 471-475.